Accepted Manuscript

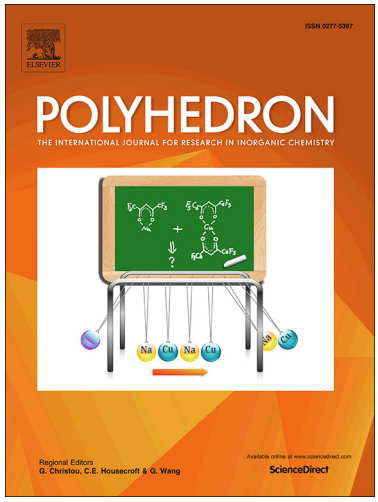

Di and Tetranuclear Cu(II) Complexes with Simple 2-Aminoethylpyridine: Magnetic Properties, Phosphodiester Hydrolysis, DNA Binding/Cleavage, Cytotoxicity and Catecholase Activity

Popuri Sureshbabu, Qazi Mohammad Junaid, C. Upadhyay, W. Victoria, Vidhyapriya Pitchavel, Sakthivel Natarajan, S. Sabiah

PII: S0277-5387(19)30108-1
DOI: https://doi.org/10.1016/j.poly.2019.02.015
Reference: POLY 13759

To appear in: *Polyhedron*

Received Date: 21 September 2018
Revised Date: 29 January 2019
Accepted Date: 1 February 2019

Please cite this article as: P. Sureshbabu, Q. Mohammad Junaid, C. Upadhyay, W. Victoria, V. Pitchavel, S. Natarajan, S. Sabiah, Di and Tetranuclear Cu(II) Complexes with Simple 2-Aminoethylpyridine: Magnetic Properties, Phosphodiester Hydrolysis, DNA Binding/Cleavage, Cytotoxicity and Catecholase Activity, *Polyhedron* (2019), doi: https://doi.org/10.1016/j.poly.2019.02.015

Di and Tetranuclear Cu(II) Complexes with Simple 2-Aminoethylpyridine: Magnetic Properties, Phosphodiester Hydrolysis, DNA Binding/Cleavage, Cytotoxicity and Catecholase Activity

Popuri Sureshbabu,[a] Qazi Mohammad Junaid,[a] C. Upadhyay,[b] W. Victoria,[a] Vidhyapriya Pitchavel,[c] Sakthivel Natarajan[c] and S. Sabiah[a]*

[a]*Department of Chemistry, Pondicherry University, Pondicherry – 605 014, India.*

[b]*School of Materials Science and Technology, Indian Institute of Technology (BHU) – 221005, India,*

[c]*Department of Biotechnology, Pondicherry University, Puducherry – 605 014, India.*

**Email. sabiahs@gmail.com*

Abstract

Di and tetranuclear Cu(II) complexes, $[Cu_2(2\text{-}AEP)_4(\mu\text{-}Cl)](ClO_4)_3$ (**1**) and $[Cu_4(\mu_3\text{-}OH)_2(\mu_2\text{-}OH)_2(2\text{-}AEP)_4(\mu_2\text{-}ClO_4)_2](ClO_4)_2$ (**2**), with the simple 2-aminoethylpyridine (2-AEP) ligand have been synthesized and characterized by different spectroscopic and analytical techniques. The X-ray structure reveals that complex **1** is a dimer with a monochloro bridge connecting the two copper atoms and complex **2** is a tetramer with μ_2 and μ_3 hydroxo bridges connecting the four copper atoms. Both copper centers in complex **1** have a distorted square pyramidal (sp) geometry, whereas two copper centres show a sp geometry and the other two copper centres show a distorted octahedral geometry in complex **2**. Variable temperature magnetic susceptibility analysis reveals that complex **1** shows a ferromagnetic interaction with 2J = +1.73 cm^{-1}, whilst **2** shows predominantly antiferromagnetic interactions between the copper(II) ions with J_1 = +2.98 and J_2= -16.91 cm^{-1}. Both complexes **1** and **2** hydrolyze the phosphodiester BNPP with rate constants k = 9.65 × 10^{-3} and 1.42 × 10^{-2} s^{-1} in CH_3CN/H_2O, respectively. These complexes interact with DNA as evidenced by theoretical and experimental methods. The DNA *in silico* study suggests that complexes **1** and **2** bind with CT-DNA through minor groove interactions, which is further confirmed by UV-Vis spectroscopic titrations, CD measurements, viscosity studies and electrochemical methods. The binding interaction of both

complexes with calf thymus DNA shows efficient binding with K_b values of 3.54×10^4 M^{-1} for **1** and 3.18×10^4 M^{-1} for **2**. Both complexes proficiently cleave plasmid DNA (pBR322) to the linear form (form III) at 25 μM under oxidative conditions and both exhibit moderate cytotoxic activity on cervical cancer cell lines (ME-180 and SiHa). In addition, both complexes catalyze the oxidation of 3,5-di-tert-butylcatechol (3,5-DTBC) to 3,5-di-tert-butylquinone (3,5-DTBQ), as studied by UV-Vis spectroscopic titrations. The rate of the reaction is 1.47×10^{-3} M s^{-1} for **1** and 3.45×10^{-3} M s^{-1} for **2**. The present complexes, with the simple 2-AEP ligand, show diverse bio-inorganic aspects.

Keywords: 2-Aminoethylpyridine, BNPP hydrolysis, DNA binding, tetranuclear copper, cytotoxicity, catecholase activity.

1. Introduction

Di and multinuclear metal complexes with bridging oxo, hydroxo, chloro and carboxylate ligands have been comprehensively studied to understand structural as well as magnetic properties.[1] Since several type 3 copper metalloproteins and non-heme iron centers have similar bridging motifs, di/multinuclear complexes with bridging ligands are considered as bio-inspired structural motifs.[2,3] Especially, a bridging moiety with a nucleophilic nature is suitable for attacking the phosphorus atom of phosphodiesters.[4-6] Hence, the hydrolytic or oxidative cleavage of phosphoesters by multinuclear copper complexes has gained much attention.[7-9] Since DNA contains phophodiester bonds, these complexes can also be viewed as targets for nucleic acid chemistry.[7-9] In that sense, their interaction and binding of DNA have received greater interest, partly due to their redox nature, lewis acidity, pharmacological activity and bio-relevance.[10-12] Apart from this, di/tetra copper complexes with a bridging motif are well suited for magnetostructural correlation *via* super exchange pathways.[13] They may show ferromagnetic or

antiferromagnetic behavior, depending on the bridging ligand, geometry at the metal center, Cu–Cu distance and Cu–L$_{(Bridge)}$–Cu angles.[13] Although many complexes have been reported with di hydroxo bridging ligands,[14, 15] mono chloro bridged dimers and tetrahydroxo bridged tetramers are less studied with regard to magneto-structural chemistry, especially complexes with bidentate N-donor ligands. Apart from this, bi/multinuclear copper complexes are often explored as catecholase models to convert catechols to their corresponding *ortho*-quinones.[16-22]

By considering these facts, we are interested to synthesize bi and multinuclear copper complexes with the simple 2-aminoethyl pyridine (2-AEP) ligand, with bridging hydroxyl and chloride ligands. In this perspective, we have successfully synthesized two homoleptic di and tertanuclear copper (II) complexes, $[Cu_2(2\text{-}AEP)_4(\mu\text{-}Cl)](ClO_4)_3$ (**1**) and $[Cu_4(\mu_3\text{-}OH)_2(\mu_2\text{-}OH)_2(2\text{-}AEP)_4(\mu_2\text{-}ClO_4)_2](ClO_4)_2$ (**2**). These complexes show intraferromagnetic (**1**) and antiferromagnetic (**2**) interactions *via* the bridging ligands. Both complexes are effective towards phosphodiester hydrolysis, DNA binding/cleavage and catecholase activit, and they show anticancer activity against ME-180 and SiHa cancer cell lines. The results obtained from these studies are elaborated in the present paper.

2. Results and discussion

2.1. Synthetic aspects of the copper complexes

In the present study, the simple, cheap and readily available bidentate ligand 2-aminoethylpyridine (2-AEP) was used for complexation with Cu(II) salts. The reaction of 2-AEP with copper(II) chloride dihydrate ($CuCl_2.2H_2O$) and copper(II) perchlorate hexahydrate ($Cu(ClO_4)_2.6H_2O$) in a 1:1 ratio yielded di and tetranuclear copper(II) complexes **1** and **2** in good yields, as illustrated in Scheme 1. Although the PF_6 analogue of 2-AEP is known, its synthesis was entirely different from that in the present work.[23e] Complexes **1** and **2** were found to be air and moisture stable and are soluble in common solvents like DMSO, DMF, CH_3CN and H_2O.

These complexes are partially soluble in MeOH. Both complexes were characterized by spectroscopic (UV-Vis, FT-IR and EPR) and elemental analyses. Variable temperature magnetic susceptibility studies were investigated to understand the magnetic nature of these bridged copper complexes. Structurally characterized dinuclear copper(II) complexes containing a single chloro bridge with bidentate ligands are scant in the literature. Only nine examples are known with bidentate ligands, and their magnetic data were not available.[23, 43]

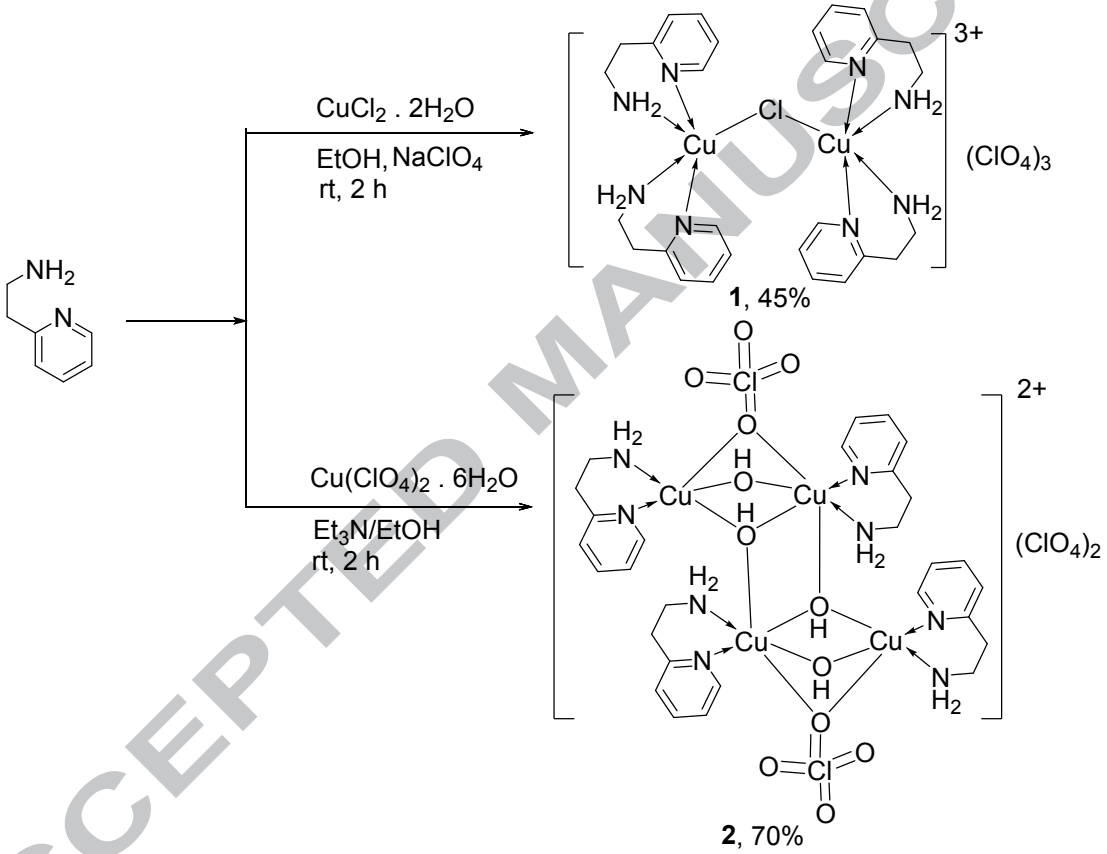

Scheme 1. Synthetic pathway for the di and tetranuclear copper complexes **1** and **2**.

2.2. Structural description of 1 and 2

2.2.1. Complex 1: Complex **1** was crystallized from an acetonitrile/methanol mixture as blue crystals in the monoclinic system with the *C* 2/*c* space group [Fig. 1a]. The asymmetric unit of complex **1** consists of one Cu(II) ion, two 2-AEP ligands, one coordinated chloride anion (Cl^-) and two perchlorate anions [Fig. 1b]. There is an inversion centre within the molecule. The two

Cu(II) centers are connected by a singly bridging chloride anion to form a dinuclear unit having the molecular formula $[Cu_2(2\text{-AEP})_4(\mu\text{-Cl})](ClO_4)_3$. Both Cu(II) centres are in a distorted square pyramidal (sp) geometry, with contributions from four nitrogen atoms of the two 2-AEP ligands and the fifth coordinating site being occupied by the mono bridged chloride anion (Fig. 1(c)). The geometry on each copper(II) ion could be best described with the geometric parameter τ (trigonality index) whose value suggests a square pyramidal geometry when τ is close to zero and a trigonal bipyramidal geometry when τ is close to 1.[24] For complex **1**, τ = 0.35 at both the Cu1 and Cu2 atoms, and hence the geometry around the metal centers is considered as distorted square pyramidal. The two copper(II) ions are separated from each other by 5.280 Å, which is longer than for the PF_6 analogue.[23e] The average Cu-N bond length of 2.028 Å (Table 2) is comparable with the values reported for other dinuclear Cu(II) amine complexes.[25-27] Complex **1** exhibits moderate H-bonding between the hydrogen atoms on the NH_2 and aliphatic CH_2 groups and the perchlorate oxygen atoms, which stabilize the structure {C-H6···O4 (2.705 Å) and NH2···O3 (1.990 Å); O(4)···H(6b)-C(6) = 146.77° and O(3)···H(4B)-N(4) = 159.91°}.

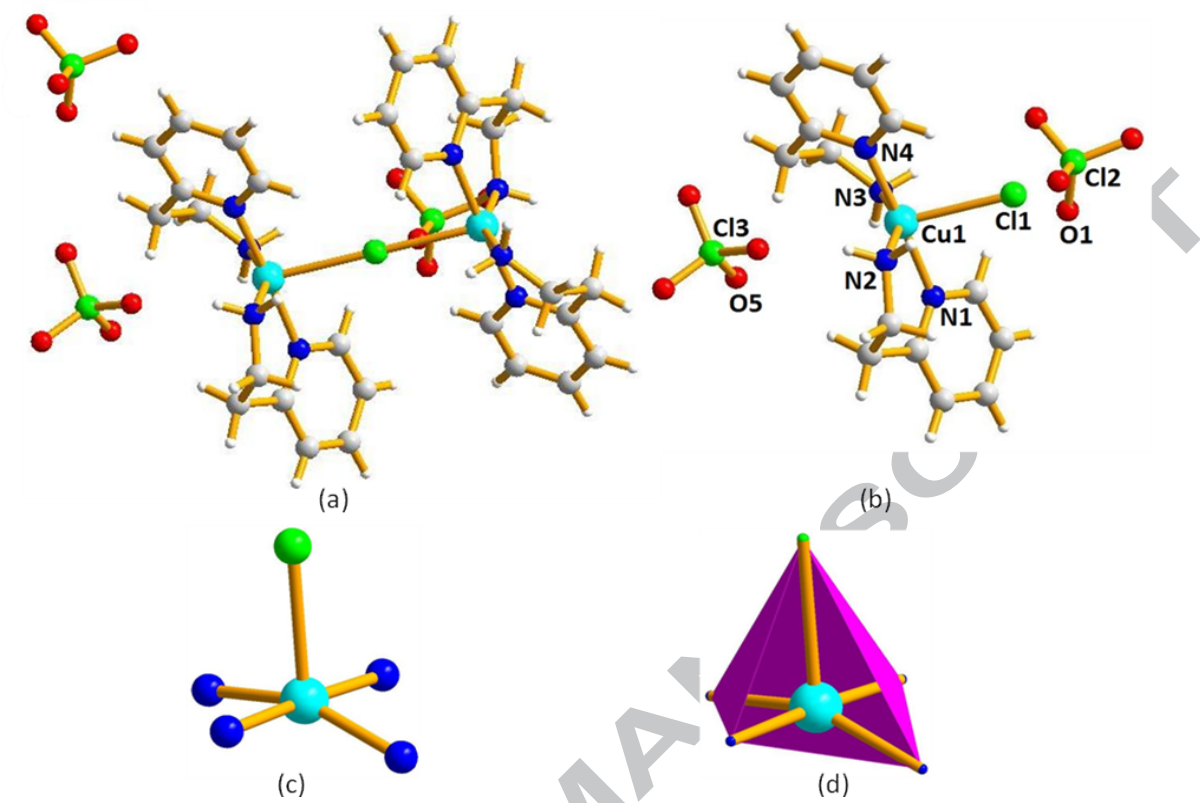

Fig. 1. (a) Crystal structure of complex **1**. (b) Asymmetric unit. Color code: H, C (grey), N (blue), Cl (green) and Cu (cyan). (c) Distorted square pyramidal (SP) geometry around the copper(II) ion. (d) Polyhedral view of the SP geometry.

2.2.2. Complex 2: Complex **2** was crystallized from acetonitrile solvent as blue crystals. Single crystal XRD analysis shows a triclinic system with the P-1 space group. The asymmetric unit of complex **2** consists of two copper(II) ions, two AEP ligands, two coordinated hydroxyl groups, one perchlorate ligand and one perchlorate anion [Fig. 2a].

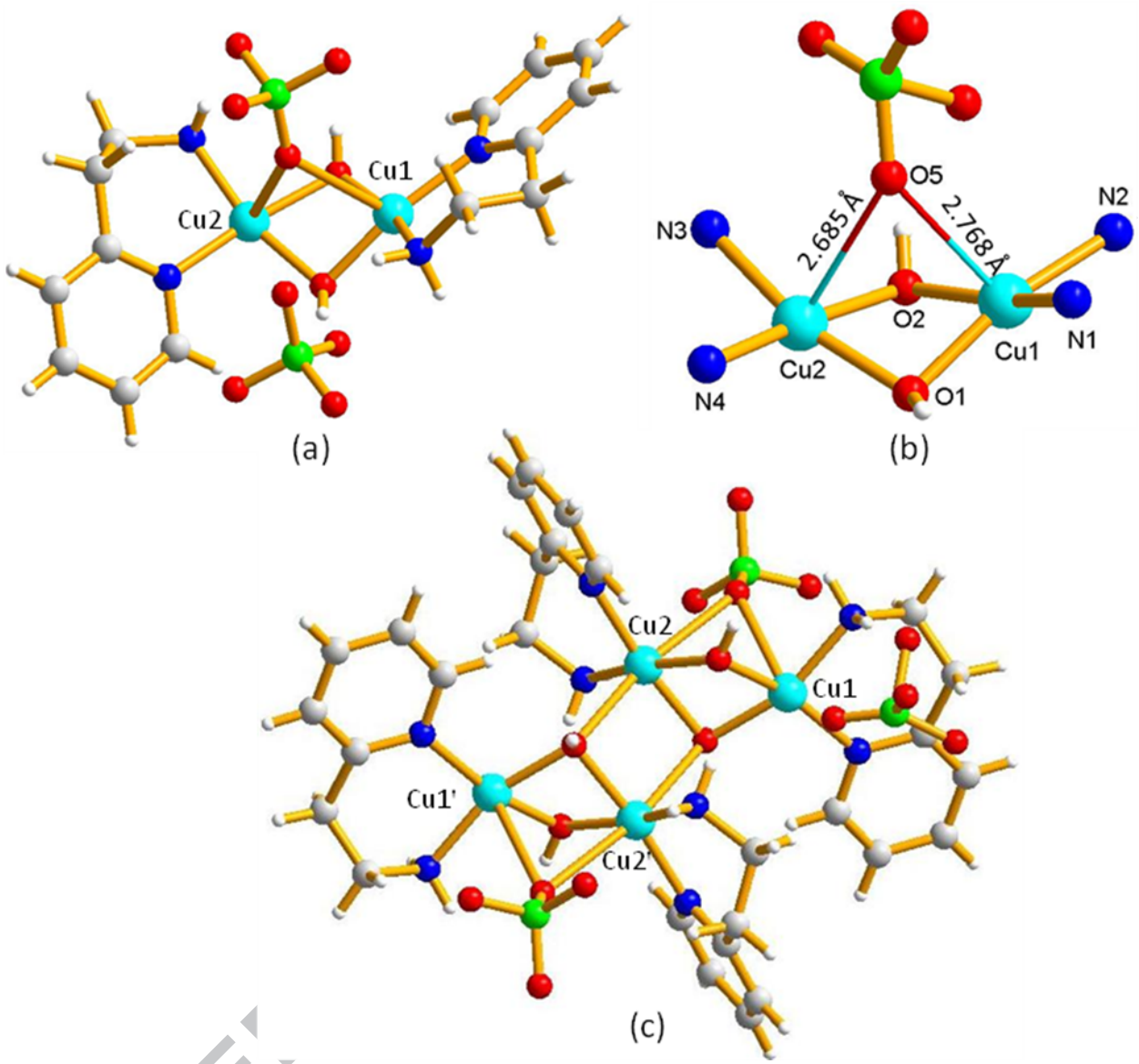

Fig. 2. Diamond view. (a) Asymmetric unit of complex **2**. Color code: H, C(grey), N (blue), O (red), Cl (green) and Cu (cyan). (b) Typical distorted SP geometry around the Cu_1(II) ion (one dimer unit). (c) Crystal structure of **2**.

Both Cu(II) centers have different spacial arrangements , namely like five coordination at Cu_1(II) and six coordination at Cu_2(II) by 2-AEP N donor atoms, four bridging hydroxyls (two μ_2-OH and two μ_3-OH) and a bridging perchlorate oxygen atom, resulting in typical distorted square pyramidal and octahedral geometries [Fig. 2b]. Hence the tetrameric unit has the formula $[Cu_4(\mu_3\text{-}OH)_2(\mu_2\text{-}OH)_2(2\text{-}AEP)_4(\mu_2\text{-}ClO_4)_2](ClO_4)_2$ (Fig. 2c). The geometric parameter τ = 0.06

at the Cu1 atom supports the square pyramidal geometry around the Cu_1(II) center in complex **2**. The Cu---Cu distances vary from 2.872 to 6.161 Å. An effective interaction is seen between the Cu1 and Cu2 atoms, with a separation of 2.872 Å. The average Cu-N bond length of 2.018 Å (Table 2) is comparable with the values reported for other tetranuclear Cu(II) N-donor complexes.[25-27] Many hydrogen bonds exist between the nitrogen bonded hydrogen atoms of 2-AEP and the oxygen atoms of the perchlorate anions, which stabilize the structure. Packing diagrams of complexes **1** and **2** are shown in Fig. 3.

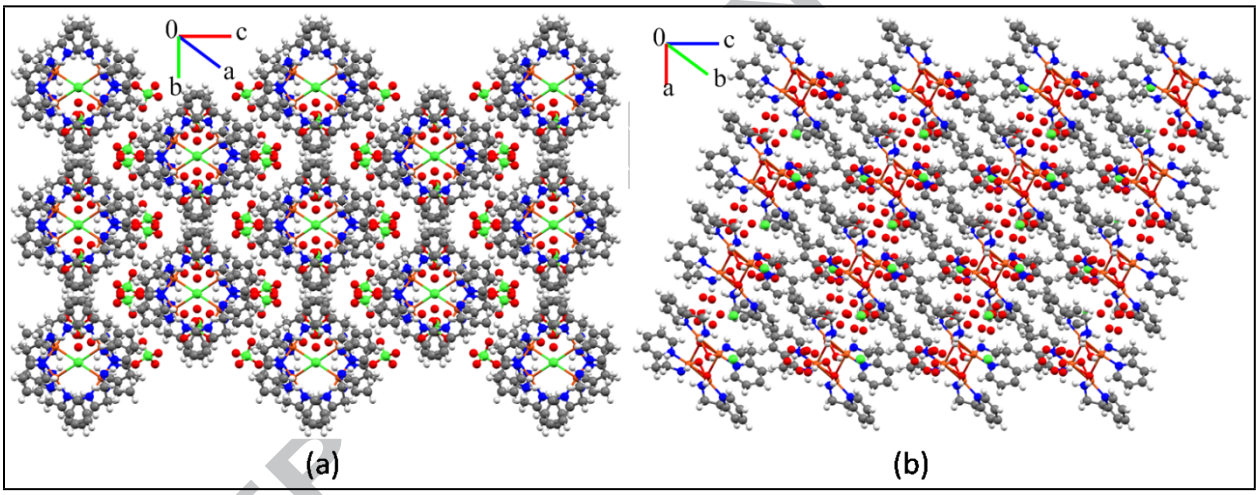

Fig. 3. Illustration of the crystal packing diagrams in two dimensional sheets of (a) complex **1**, viewed along the c-axis, and (b) complex **2**, viewed along the b-axis.

Table 1. Crystal parameters for **1** and **2**

Parameters	**1**	**2**
CCDC	1567730	1567729
Molecular formula	$C_{28}H_{40}Cl_4Cu_2N_8O_{12}$	$C_{28}H_{44}Cl_4Cu_4N_8O_{20}$
Molecular weight	949.56	1208.68
Crystal system	Monoclinic	Triclinic
Space group, Z	C 2/c, 4	P-1, 1
a (Å)	21.975(8)	8.846(5)
b (Å)	12.215(3)	11.236(7)
c (Å)	15.288(6)	12.663(8)
α (°)	90	112.305(6)
β (°)	105.847(4)	105.254(5)
γ (°)	90	95.851(5)
V ($Å^3$)	3948.2(2)	1094.39(13)
Temperature (K)	293(2)	293(2)
λ (Å)	0.71073	0.71073
D_c (Mg/m^3)	1.597	1.834
μ (mm^{-1})	1.415	2.247
Reflections collected	3867	5041
Reflections used	2921	3593
No.of refined parameters	276	394
$^aR_1$ [1>2σ(I)]	0.1682	0.0759
$^bR_{2w}$	0.1867	0.0851
Goodness of fit	1.034	1.0671

$^aR_1=\Sigma||F_o| -|F_c||/\Sigma|F_o|$, $^bwR_2=|\Sigma_w(|F_o|^2-|F_c|^2)|/\Sigma|w|(F_o)^2|^{1/2}$

Table 2. Selected bond lengths (Å) and angles (°) of $[Cu_2(2\text{-AEP})_4(\mu\text{-Cl})](ClO_4)_3$ (**1**) and $[Cu_4(\mu_3\text{-OH})_2(\mu_2\text{-OH})_2(2\text{-AEP})_4(\mu_2\text{-}ClO_4)_2](ClO_4)_2$ (**2**)

Complex 1							
Bond lengths (Å)				**Bond angles (°)**			
Cu1-N1	2.036	Cu1-N4	2.011	N1-Cu1-N2	89.41	N3-Cu1-N4	93.10
Cu1-N2	2.030	Cu1-Cl	2.640	N1-Cu1-N3	177.31	N1-Cu1-Cl	95.01
Cu1-N3	2.036	Cu1- Cu1	5.280	N1-Cu1-N4	86.90	N2-Cu1-Cl	109.85
				N2-Cu1-N3	89.51	N3-Cu1-Cl	87.68
				N2-Cu1-N4	156.17	N4-Cu1-Cl	93.93
Complex 2							
Bond lengths (Å)				**Bond angles (°)**			
Cu1-N1	2.024	Cu1-O5	2.768	N1-Cu1-N2	95.32	N3-Cu2-O2	163.00
Cu1-N2	1.989	Cu2-O5	2.685	N1-Cu1-O1	172.36	N4-Cu2-O1	162.59
Cu1-O1	1.966	Cu1- Cu2	2.873	N1-Cu1-O2	96.22	N4-Cu2-O2	92.92
Cu1-O2	1.941	Cu1- Cu1'	3.167	N2-Cu1-O1	91.44	Cu1-O1-Cu2	93.02
Cu2-N3	2.029	Cu1- Cu2'	3.968	N2-Cu1-O2	166.37	Cu1-O2-Cu2	95.85
Cu2-N4	1.970	Cu1'- Cu2'	2.873	N3-Cu2-N4	95.00	O1-Cu1-O2	76.64
Cu2-O1	1.964	Cu2- Cu1'	3.968	N3-Cu2-O1	97.83	O1-Cu2-O2	76.67
Cu2-O2	1.929	Cu2- Cu2'	6.161				

3. Spectral characterization

The synthesized copper(II) complexes **1** and **2** were further characterized by UV-Vis, FT-IR, EPR and cyclic voltammetric techniques.

3.1. UV-Vis spectra

The UV-Vis spectra of complexes **1** and **2** were recorded in acetonitrile at RT in the spectral window 190-1100 nm and are illustrated in Fig. 4. The absorption spectrum of the mono-chloro bridged complex **1** displayed a broad lower energy band centered around 735 nm (ε = 206 $M^{-1}cm^{-1}$), corresponding to the d-d transition of a Cu(II) ion in a square pyramidal geometry. Complex **2** displayed a d-d transition around 608 nm (ε = 294 $M^{-1}cm^{-1}$), similar to other hydroxo bridged Cu(II) complexes.[28, 29]

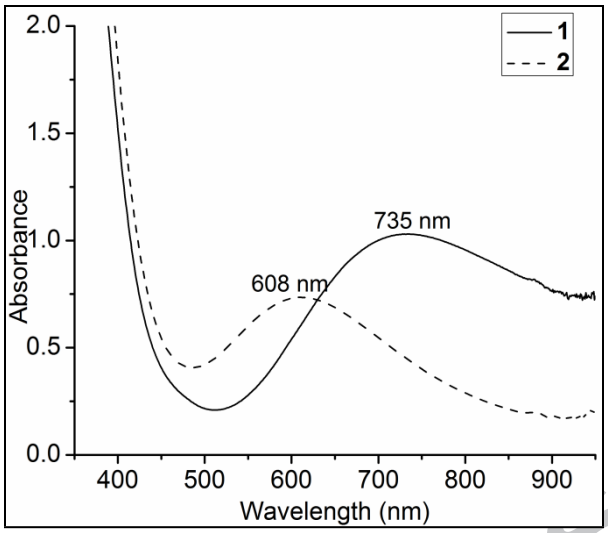

Fig. 4. The UV-Vis spectra of the di and tetranuclear copper complexes **1** (5 mM) and **2** (2.5 mM) in acetonitrile.

3.2. Infrared (FT-IR) spectra

The FT-IR spectra of complexes **1** and **2** were recorded at room temperature in the region 4000-400 cm^{-1}. Complexes **1** and **2** exhibited a characteristic band at 3314-3447 cm^{-1} ascribed to $\nu_{(NH2)}$ coordinated to copper(II) centers.[30, 31] The sharp bands around 3107-3214 cm^{-1} were due to $\nu_{(=CH)}$ stretching vibrations of pyridine groups and those in the range 2917-2924 cm^{-1} were due to $\nu_{(CH2)}$ vibrations of the aliphatic methylene groups. In addition to these bands, the complexes displayed strong bands around 1080-1088 and 623-630 cm^{-1} due to perchlorate group asymmetric stretching and bending modes respectively. Complex **2** displayed a broad characteristic envelop at 3482 cm^{-1} due to bridging OH groups.

3.3. EPR spectra

The solid state EPR spectra of complexes **1** and **2** were recorded with a magnetic field strength of 2000-4500 G (Fig. 5) at room temperature. The spectra revealed two signals, indicating tetragonally distorted Cu(II) centers with $g_{\|}$= 2.27 and $g_{\perp}$= 2.05 for **1**, and $g_{\|}$= 2.25 and $g_{\perp}$= 2.06 for **2**. The obtained values match with those of distorted Cu(II) environments in similar complexes.[32]

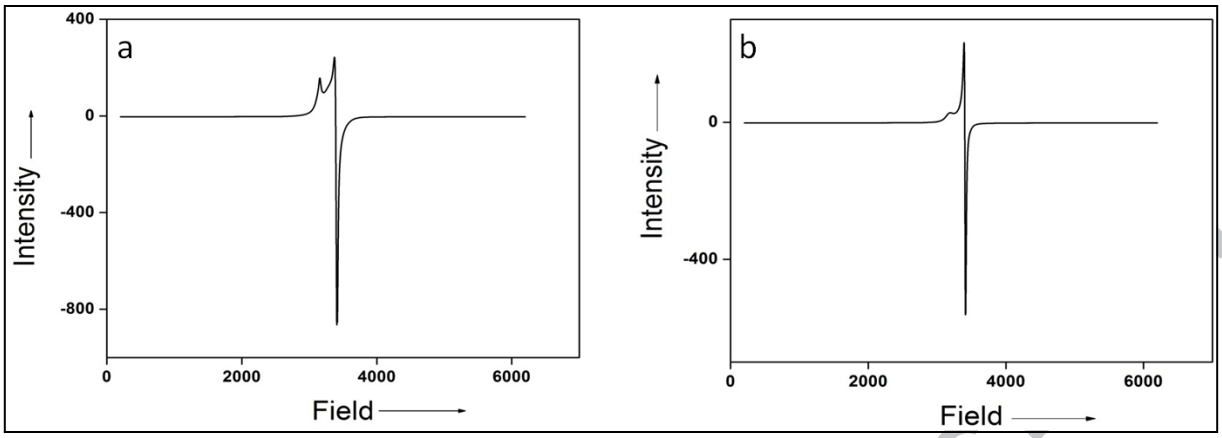

Fig. 5. EPR spectra of (a) $[Cu_2(2\text{-}AEP)_4(\mu\text{-}Cl)](ClO_4)_3$ (**1**), (b) $[Cu_4(\mu_3\text{-}OH)_2(\mu_2\text{-}OH)_2(2\text{-}AEP)_4(\mu_2\text{-}ClO_4)_2](ClO_4)_2$ (**2**), at room temperature, scan range = 2000–4500 G, mod. amplitude = 5 G and microwave frequency = 9.40715 GHz.

3.4. Magnetic studies

Magneto-structural correlations of di and multinuclear complexes with bridging ligands often gained attention to understand super exchange pathways. Especially, tetra-copper complexes with μ-hydroxo systems and bidentate ligands were studied by a few groups.[33] The magneto-structural correlation of complexes with a singly bridging chloride ion and bidentate ligands is still a matter of investigation. Hence we have carried out a magnetic susceptibility study on the present complexes.

The magnetic susceptibility studies of complexes **1** and **2** were carried out on crystalline samples in the temperature range 2-300 K. The magnetic responses are illustrated in Figs. 6 and 7. The magnetic behaviour of both complexes have been analyzed using the modified Bleaney-Bowers equation (3.4.1),[34a,b] where g is the magnetic field splitting factor, J is the exchange parameter with +J and -J indicating ferromagnetic and antiferromagnetic exchange interactions between two Cu(II) ions, respectively. TIP is the temperature independent paramagnetism contribution of 1 mole of copper(II) ions. The modified Bleany-Bowers equation used for fitting the obtained data is given by eq 3.4.1.

$$\chi_m = \frac{2N_A g^2 \beta^2}{3K_B(T-\theta)}\left[1+1/3\exp(-2J/K_BT)\right]^{-1} + TIP \cdots\cdots\cdots\cdots\cdots\cdots (3.4.1)$$

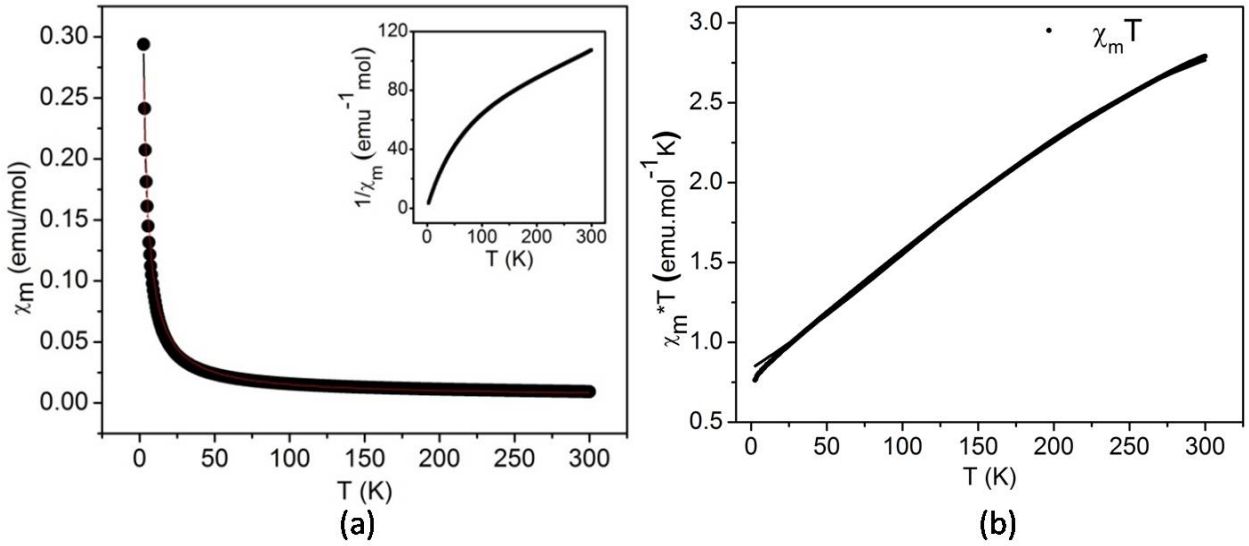

Fig. 6. Plot (a) χ_m*vs* T (b) χ_mT*vs* T in the range 2-300 K for **1** (inset $1/\chi_m$*vs* T) (the solid line indicates the theoretical curve from the Bleaney-Bowers equation).

The obtained data for complexes **1** and **2**, in the form of molar magnetic susceptibility (χ_m) versus temperature (T) and $1/\chi_m$ versus temperature (T), are shown in Figs. 6 and 7a. From the strong deviation in the plot, it was proposed that complex **1** displays a dual nature (ferro and antiferromagnetism) with respect to temperature. The fitting of the obtained data in the equation (3.4.1) in the higher temperature range for complex **1** showed ferromagnetic-like behaviour (2J = +1.73 cm^{-1}), whereas the lower temperature range showed antiferromagnetic nature (2J = -13.48 cm^{-1}). At lower temperatures, intermolecular antiferromagnetic interactions or zero field splitting might have an influence on the structure of the complex.[35, 36] However, the positive *J* value suggests an intramolecular ferromagnetic exchange interaction between the two copper(II) centers. The χ_mT values for **1** at 300 and 50 K are 2.8 and 1.18 cm^3 mol^{-1} K, respectively. A superexchange interaction in complex **1** is possible through the chloride bridge between the Cu(II) centers. The exchange interaction between the two copper(II) ions mainly depends on the

Cu···Cl···Cu bridging angle, together with the Cu···Cu and Cu···Cl distances.[37] The magnetic parameters obtained from the fitting of data using eq 3.4.1 are listed in Table 3 and compared with available complexes in Table 4. From Table 4, it is clear that only a limited number of mono chloro bridged dicopper complexes are available with bidentate N-donor ligands. Unfortunately, the J values are not available for these complexes to bring about any meaningful magneto structural correlation.

The equations used for fitting the obtained data for tetranuclear complex **2** are given below:[34c]

$$\chi_{exp} = (1-\rho)\chi_{complex} + \rho\chi_{imp} + TIP$$

$$\chi_{exp} = \frac{2N\beta^2g^2}{kT} \{[2\exp(-y) + \exp(-x) + 5\exp(x)] / [\exp(-2y) + 6\exp(-y) + \exp(-2x) + 3\exp(-x) + 5\exp(x)]\} \quad \text{.....(3.4.2)}$$

$$\text{with} \quad x = \frac{J_1}{kT} \quad \text{and} \quad y = \frac{J_2}{kT}$$

The magnetic properties of complex **2**, in the form of molar magnetic susceptibility (χ_M) versus temperature (T) and $1/\chi_m$ versus temperature (T) plots, are shown in Fig.7. The inset of Figure 7(a) shows the residual plot of the measured and fitted data. The difference between the measured and fitted data is ~ 1%, showing the goodness of the fitting. The χ_mT values for complex **2** at 300 and 50 K are 1.08 and 1.05 $cm^3\ mol^{-1}\ K$; J_1 = +2.98 and J_2= -16.91 cm^{-1}. In general, the magnetic susceptibility was influenced by several factors, such as the geometry around the copper center, Cu-O(H)-Cu angle, Cu-O bond distances and Cu-Cu bond lengths. Among these, the Cu-O(H)-Cu angle plays a major role for spin coupling between copper centers, with S = ½.[37] Hence, ferromagnetism is observed when the Cu−O(H)−Cu angles are smaller than 97.5° due to accidental orthogonality of the magnetic orbitals and antiferromagnetism is observed at higher angles, especially in dihydroxo bridged dicopper(II) complexes[38, 39] Ruiz *et al*., explained the two possible mechanistic pathways for the exchange

interaction in bis-μ-hydroxo di and tetranuclear copper(II) complexes: 1) direct interaction between Cu(II) ions, 2) superexchange interaction propagated through the hydroxyl bridge.[40] The observed Cu1−O1(H)−Cu2 angle of 95.7° and Cu1−O2(H)−Cu2 angle of 92.9°, with a positive J_1 = +2.98 value (Table 3), suggest a ferromagnetic interaction. At the same time, the J_2 value of -16.91 cm^{-1} suggests the dominance of an antiferromagnetic interaction. The magneto structural correlation of selected hydroxo bridged tetracopper complexes with bidentate ligands is shown in Table 5. From the table, it is visible that complex **2** shows a moderate antiferromagnetic interaction, comparable with the reported complexes.

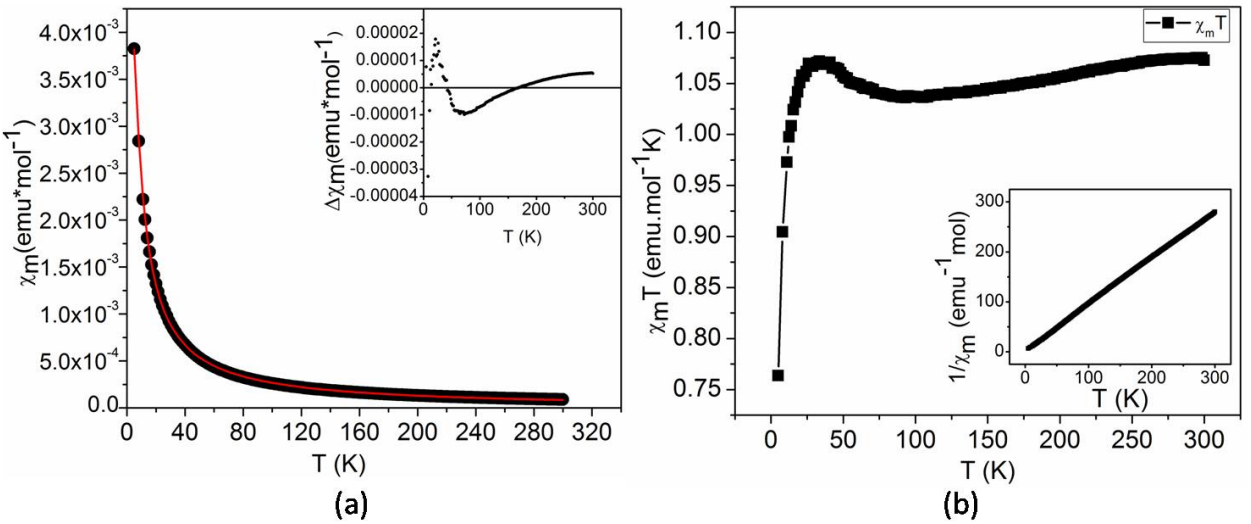

Fig. 7. Plot of (a) χ_m*vs* T (b) χ_mT*vs* T in the range 2-300 K for **2** (the solid line indicates the fitted curve using the Bleaney-Bowers equation).

Table 3. Selected magnetic data for di and tetranuclear bridged copper(II) complexes

Complex	T (K)	exchange parameter (cm^{-1})	Θ (Kelvin)	g	TIP (cm^3 /mol)	Impurities (%)	R^2
1	2-300	2J=+1.73	-2.13	2.15	5 x 10^{-6}	0.005	0.99
2	2-300	J_1 = +2.98 J2 = -16.91	-3.99	2.12	5 x 10^{-6}	0.01	0.99

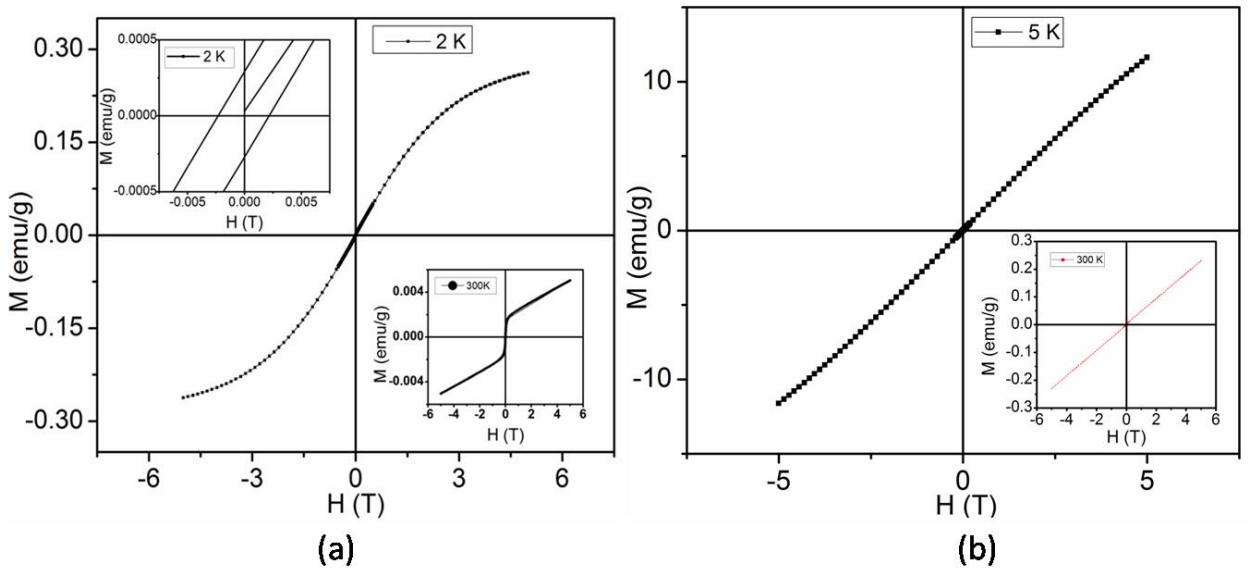

Fig.8. Magnetization *vs* applied field curve for (a) **1** and (b) **2**. Right bottom inset shows the M-H plot at 300 K and left top shows the M-H plot at the lowest temperature.

The obtained magnetic susceptibility data for complexes **1** and **2** can also be correlated by their M-H curves. The M-H behavior of both complexes is distinct, as shown in Fig.8. In the case of complex **1**, the M-H plot at 2 K showed a non-linear ferromagnetic hysteresis curve with an remanence of 3 x 10^{-4} emu/g and coercivity of 23 Oe (as shown in the top left inset), whereas we observed that the M-H plot at 300 K (as shown in the inset) behaved like a complex antiferromagnetic system, having a non-saturating magnetization, even at an applied field of 5 T. This further confirmed our assignment of a ferromagnetic to antiferromagnetic like transition in complex **1**. In the case of complex **2**, the M-H behavior showed an almost linear pattern at both the temperatures 300 and 5 K. However, it also had a coercivity of 30 Oe and remanent magnetization of 7 × 10^{-3} emu/g. The value of the remanence is almost an order of magnitude higher than that of complex **1**. It may be noted that the J value was relatively high in comparison with that of complex **1**, correlating well with these observations.

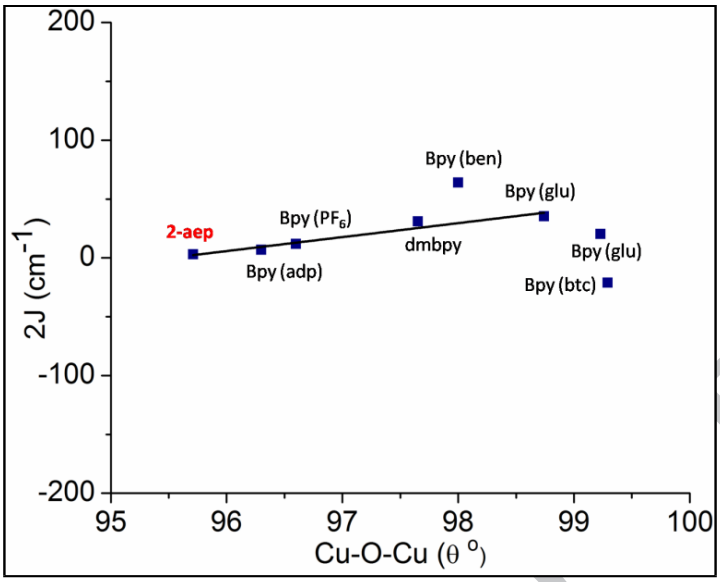

Fig. 9. The plot of *2J* vs. θ (Cu-OH-Cu) for related tetranuclear copper *bis*-μ-hydroxo bridged complexes with bidentate ligands.

The correlation of 2*J vs* θ for selected tetranuclear copper bis-μ-hydroxo complexes with bidentate ligands (selected from Table 5) is shown in Fig. 9. The correlation pattern for complex **2** falls on the linear relationship.

Table 4. Comparison of bond angles and J values for dinuclear mono-chloro bridged Cu(II) complexes with bidentate N-donor ligands.

Complex	Cu-Cl-Cu angle (°)	Cu…Cu distance (Å)	Cu…Cl distance (Å)	J value (cm^{-1})	Ref
$[Cu_2(2\text{-AEP})_4(\mu\text{-Cl})](ClO_4)_3$ (**1**)	180.00	5.280	2.640	+1.73	This work
$Cu_2(phen)_2(\mu\text{-Cl})(Cl_3)$	90.86	3.564	2.706	-	43(b)
$[Cu_2(acec)_2(bpy)_2(\mu\text{-Cl})](ClO_4)(H_2O)$	127.50	4.500	2.509	-	23(a)
$[Cu_2(2,9\text{-tb-phen})_2(\mu\text{-Cl})(Cl_3)](SbF_6)$	89.92	3.097	2.196	-	23(b)
$[Cu_2(2,5\text{-bamp})_2(\mu\text{-Cl})(Cl_3)]$	95.24	3.709	2.227	-	23(c)
$[Cu_2(tmeda)_2(\mu\text{-Cl})(CO_2)](BPh_4)$	102.96	3.643	2.306	-	23(d)
$[Cu_2(2\text{-aep})_4(\mu\text{-Cl})](PF_6)_3$	180.00	5.060	2.530	-	23(e)
$[Cu_2(maep)(\mu\text{-Cl})(Cl_2)]_n$	113.58	4.263	2.785	-	23(f)
$[Cu_2(PYP)(\mu\text{-Cl})(Cl_2)]_n$	98.64	3.785	2.701	-	23(g)
$[Cu_2(aei)(\mu\text{-Cl})(Cl_2)]_n(Cl)(H_2O)_2$	131.79	5.232	2.856	-	23(h)

Table 5. Magneto-structural correlation of selected tetranuclear bis-(μ-OH) bridged Cu(II) complexes with bidentate N-donor ligands

Complex	Cu-O-Cu angle (°)	Cu…Cu distance (Å)	Cu…O distance (Å)	J_1 (cm^{-1})	Ref
$[Cu_4(2\text{-}AEP)_4(\mu_3\text{-}OH)_2(\mu_2\text{-}OH)_2(\mu_2\text{-}ClO_4)_2](ClO_4)_2$ (**2**)	95.71(0)	2.872(0)	1.931(0)	+2.98	This Work
$[Cu_4(bpy)_4(OH)_4\ (H_2O)_2](C_8HO_4)_3.6H_2O$	96.30(0)	2.915(0)	1.930(0)	+6.79	33a
$[Cu_4(bpy)_4(OH)_4\ (H_2O)_2](NO_3)_2(C_7H_5O_2)_2.6H_2O$	98.00(0)	2.898(0)	1.919(0)	+64.1	33b
$[Cu_4(bpy)_4(OH)_4\ (H_2O)_2](NO_3)_2(C_5H_6O_4).8H_2O$	99.23(0)	2.918(0)	1.920(0)	+20.3	33b
$[Cu_4(bpy)_4(OH)_4\ (H_2O)_2](C_5H_6O_4)_2.16H_2O$	98.74(0)	2.912(0)	1.924(0)	+35.4	33b
$[Cu_4(dmbpy)_2(OH)_4(H_2O)_2](BF_4)_2\ (H_2O)_4$	97.65(0)	2.939(0)	1.973(0)	+31.1	33c
$[Cu_4(bpy)_4(OH)_4(H_2O)(BTC)]NO_3.8H_2O$	99.29(0)	2.907(0)	1.905(0)	-21.1	33d
$[Cu_4(bpy)_4(OH)_4](PF_6)_4$	96.60(2)	2.914(0)	1.947(2)	+12.0	33e

4. Phosphodiester hydrolysis

Having synthesized the di and tetranuclear copper(II) complexes, we have performed phosphodiester (PDE) hydrolysis experiments as the complexes possess hydroxo/chloro nucleophiles which are capable of attacking the electrophilic phosphorus atom of phosphodiesters. Bis(4-nitrophenyl) phosphate (BNPP) is often used as a substrate to study such reactions. When BNPP undergoes hydrolysis, the product 4-nitrophenolate (p-NP) can be detected in basic pH by its characteristic band around λ_{max} = 400 nm in UV-Vis spectra [Fig. 10a].[41]

Pseudo-first-order rate constants were determined using the initial rate method.[42a, 44c] From these preliminary studies, the rate and rate constant of BNPP hydrolysis were calculated from the slope of a linear plot of [*p*-NP] *vs* time (Figs. 10b and 11b). The rate and rate constant for complex **1** were 8.49×10^{-5} mM s^{-1} and 9.65×10^{-3} s^{-1}. Similarly, these values for complex **2** were 9.79×10^{-5} mM s^{-1} and 1.42×10^{-2} s^{-1}, respectively. The present di and tetra-nuclear complexes showed hydrolytic activity comparable to many reported copper complexes. For instance, dinuclear copper complexes with tacn ligands bearing alkyl guanidine moieties were

reported by Leone Spiccia's group and showed hydrolytic activity k = 1.35 × 10^{-6} s^{-1}.[8b] R.E.H.M.B. Osória reported dinuclear copper(II) complexes and studied phosphodiester hydrolysis with rates of the reaction in the range 1.8 – 5.1 × 10^{-4} s^{-1}.[42b] Sabiah, *et al*. reported a dinuclear copper(II) complex for phosphodiester hydrolysis with reaction rate of 1.5 × 10^{-5} s^{-1}.[8a]

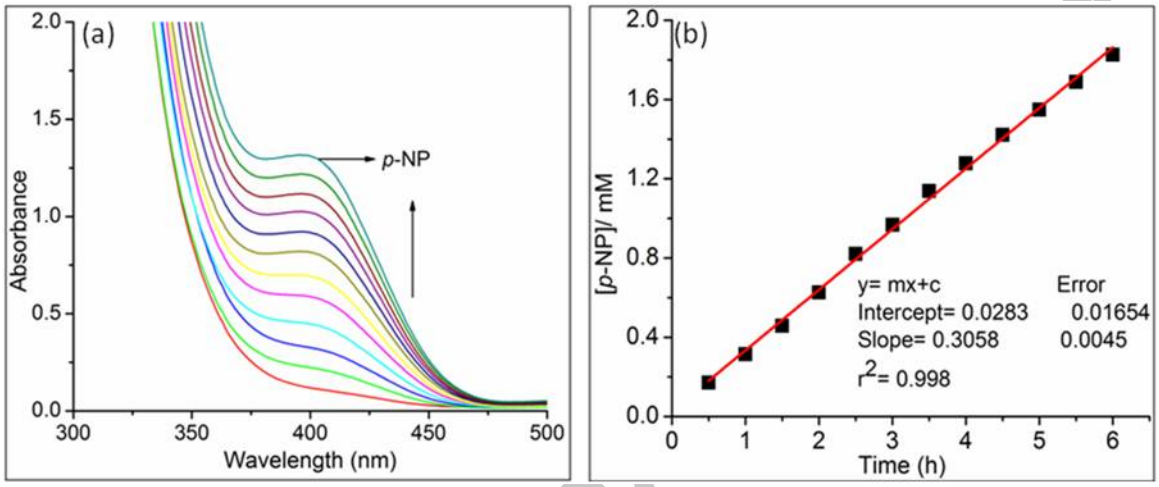

Fig. 10. (a) Spectral profile for the hydrolysis of BNPP by complex **1**. Spectra were recorded every 30 min. (b) Plot of concentration *vs* time.

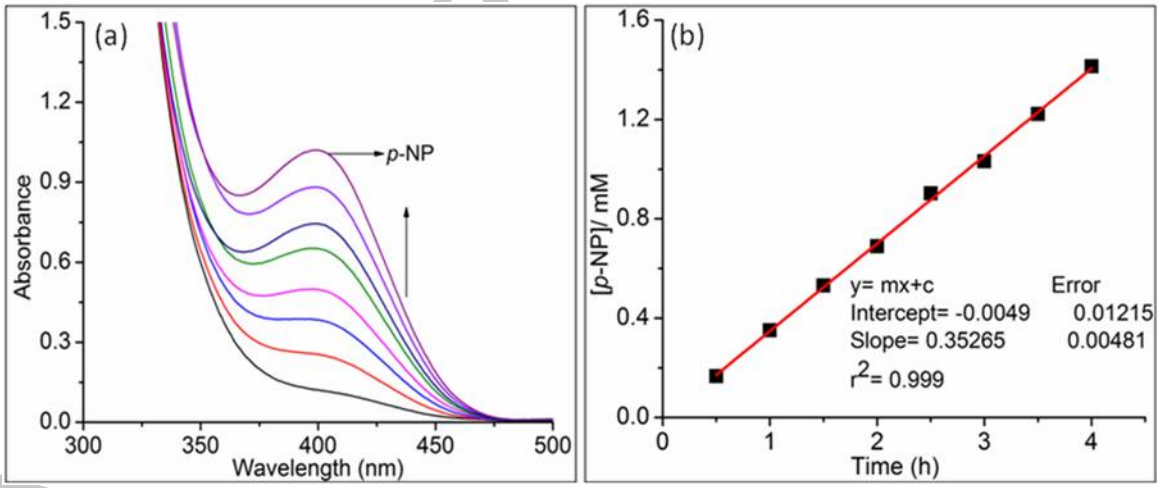

Fig. 11. (a) Spectral profile for the hydrolysis of BNPP by complex **2**. Spectra were recorded every 30 min. (b) Plot of concentration *vs* time.

5. DNA interaction studies

5.1. UV-Vis spectrophotometric study

Since we were interested in understanding the DNA binding interactions with the di and tetranuclear complexes **1** and **2**, we have carried out interaction studies using UV-Vis, FT-IR, CD and CV methods. The binding affinity of complexes **1** and **2** with calf thymus DNA (CT-DNA) was measured by electronic absorption spectroscopy as it is one of the simple, commonly employed methods to determine the binding nature of metal complexes with CT-DNA. The titrations for the present complexes were carried out by varying the concentration of CT-DNA from 0 to 20 μM and fixing the complex concentration constant (**1** = 5 mM; **2** = 2.5 mM). The absorption intensity of complexes **1** and **2** kept decreasing upon each addition of CT-DNA. The spectral profiles of complexes **1** and **2** in the presence and absence of CT-DNA are shown in Figs. 12a and 13a. The binding constants were calculated from the equation given below.[43]

$$[DNA]/|\varepsilon_a-\varepsilon_f| = [DNA]/|\varepsilon_b-\varepsilon_f|+1/K_b|\varepsilon_b-\varepsilon_f|$$

where [DNA] represents the concentration of CT-DNA, ε_a, ε_b and ε_f represents the extinction coefficients of partially bound DNA to the complex, the fully DNA bound complex and the free complex. The binding constant (K_b) for the complexes was estimated from the plot of $[DNA]/\varepsilon_a-\varepsilon_f$ *vs* [DNA], which yielded a straight line with the ratio of slope/intercept equal to the binding constant. The calculated binding affinities of the copper(II) complexes **1** and **2** are shown in Table 6. They show moderate binding affinities with CT-DNA, which were well comparable with reported values.[44]

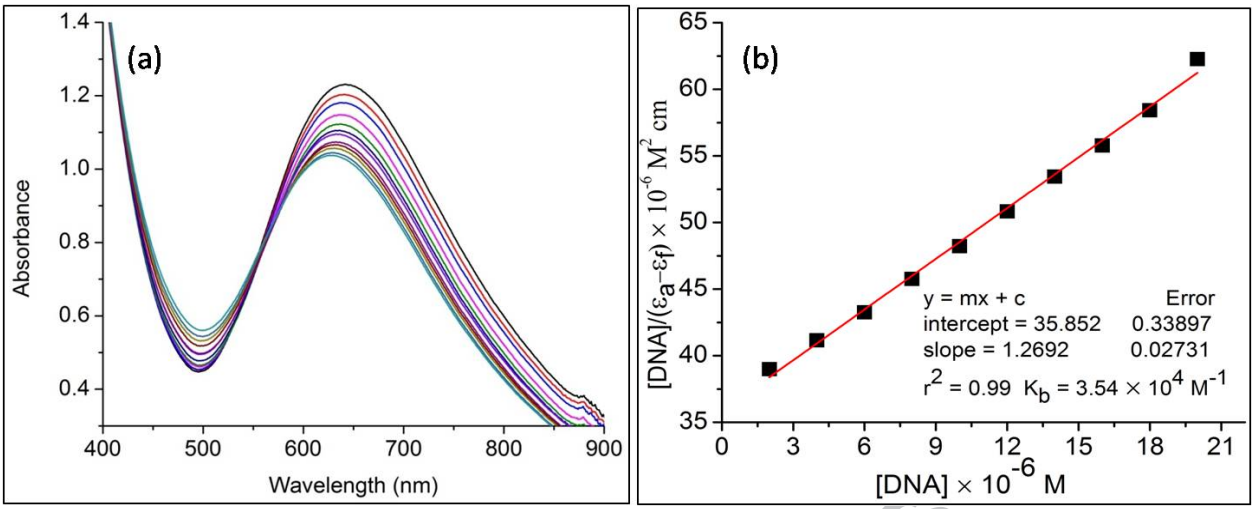

Fig. 12. (a) Spectral profile of the dinuclear copper(II) complex **1** (5 mM) with CT-DNA (0-20 µM), (b) binding plot of [DNA]/(ε_a-ε_f) *Vs* [DNA].

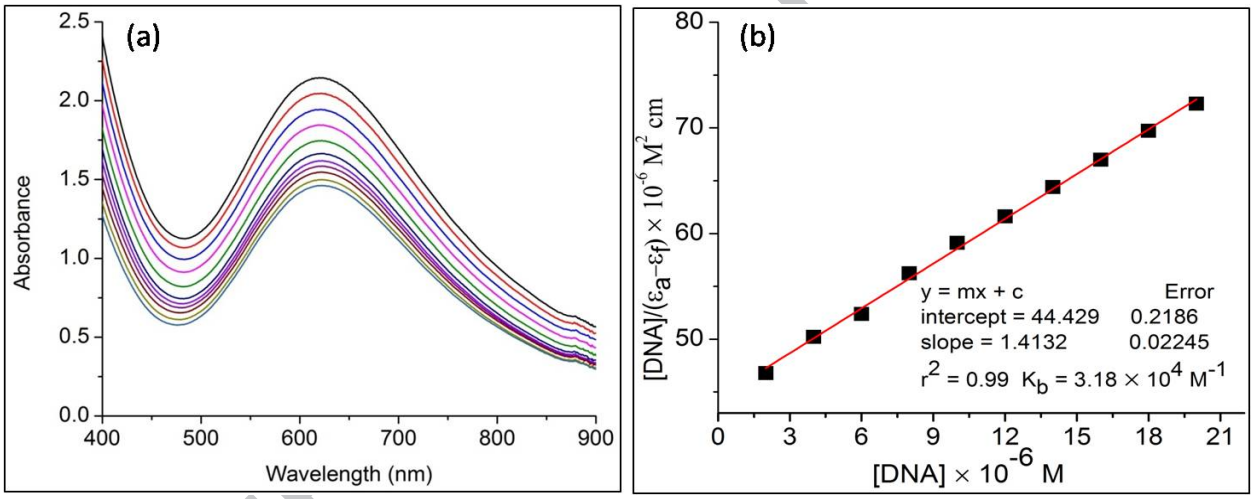

Fig. 13. (a) Spectral profile of the tetranuclear copper(II) complex **2** (2.5 mM) with CT-DNA (0-20 µM), (b) binding plot of [DNA]/(ε_a-ε_f) *Vs* [DNA].

Complexes **1** and **2** show similar binding interactions towards CT-DNA as compared to many copper complexes. For instance, N.M.R. Martins *et al*. reported dinuclear copper(II) complexes with an arylhydrazone of ethyl 2-cyanoacetate with binding constants in the range 2.7 – 3.3 × 10^5 M^{-1}.[44a] Q.Q. Zhang *et al*. reported mono chloro bridged copper complexes of phenanthroline ligands with a binding constant of 4.75 × 10^4 M^{-1}.[44b] S. Ramakrishnan *et al*. reported mixed-ligand dinuclear copper(II) complexes of a benzamide based ligand with diimine

auxiliary ligands, with binding constants in the range 0.5 – 7.6 × 10^4 M^{-1}.[44d] M. Jiang *et al*. described bridged binuclear copper(II) complexes with an oxamide ligand, having binding constants 1.73 × 10^5 M^{-1} for[Cu_2(heae)(pic)$_2$] and 1.92 × 10^5 M^{-1} for [Cu_2(heae)(Me_2phen)$_2$].[44e] Binuclear copper(II) complexes were reported by K. Zheng *et al*. with a binding constant of 8.35 × 10^5 M^{-1}.[44f] Mixed ligand copper(II) complexes of bipyridyl/phenanthroline were reported by F.-H. He *et al*., showing k_b values in the range 1.1 – 1.8 × 10^4 M^{-1}.[44g]

Table 6. Rate constants and binding constants for complexes **1** and **2**.

Complex	Phosphodiester Hydrolysis Rate constant (k) s^{-1}	DNA Binding Constant (k_b M^{-1})
[Cu_2(2-AEP)$_4$(μ-Cl)](ClO_4)$_2$ (**1**)	9.65 × 10^{-3}	3.54 × 10^4
[Cu_4(μ$_3$-OH)$_2$(μ$_2$-OH)$_2$(2-AEP)$_4$(μ$_2$-ClO_4)$_2$](ClO_4)$_2$ (**2**)	1.42 × 10^{-2}	3.18 × 10^4

5.2. FT-IR study

FT-IR spectral studies were performed to understand the binding nature between the metal complexes with nucleotides of CT-DNA. In the literature, the vibrational bands for free DNA appear at 1261, 1402 and 1639 cm^{-1}, which correspond to thymidine, cytosine and adenine bases, respectively.[45] The bands at 1087 and 991 cm^{-1} are assigned to symmetric and asymmetric stretching modes of phosphate groups respectively. After interaction of the complexes with cytosine and adenine (CT-DNA) bases, the bands are shifted to 1392 and 1627 cm^{-1} (**1**), and 1393 and 1628 cm^{-1} (**2**) respectively. These complexes also interacted with the phosphodiester moieties of DNA, as the phosphate bands shifted to 1119 and 1071 cm^{-1} (complex **1**), and 1117 and 1077 cm^{-1} (complex **2**). The obtained results strongly suggest that these complexes interact with CT-DNA *via* an electrostatic/groove binding mode.[45]

5.3. CD spectrometric study

Circular dichroism spectral studies are performed to study the interaction of molecules/metal complexes with DNA. CT-DNA was dissolved in 10 mM Tris-HCl buffer (pH 7.4) and the CD spectra of the solution showed characteristic positive and negative peaks around 285 and 240 nm due to base stacking and helicity, respectively. If any molecule/metal complex interacts with CT-DNA *via* a groove/electrostatic interaction, it will exhibit a small or no perturbation on both the helicity bands and base stacking in the spectra, where as intercalation enhances the intensities of both the bands, as well as shifting the position of the peaks. Complexes **1** and **2** were incubated along with CT-DNA at [DNA]:[complex] ratios of 1:0.5 (**1**) and 1:0.25 (**2**) ratio, and the spectra were recorded at ambient temperature in 10 mM buffer solution. The obtained spectra revealed that there was a small change in the intensities of both the negative and positive bands, but there was no considerable shift in the peaks (Fig. 14). Hence, the results suggested that both copper complexes bind with CT-DNA *via* the groove mode.[46]

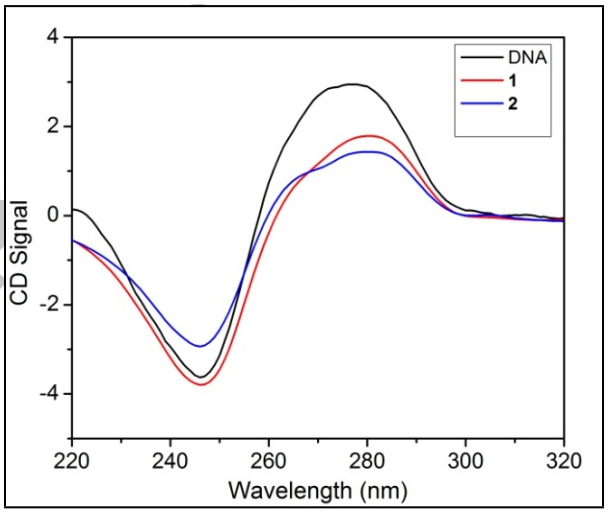

Fig. 14. CD spectral profile of CT-DNA with **1** and **2** in 7.4 pH buffer at room temperature, where [CT-DNA]:[complex] = 1:0.5 (**1**) and 1:0.25 (**2**).

5.4. Viscosity measurements

A viscosity study is a simple, often used and effective method to find the mode of binding between complexes and CT-DNA.[46] Generally this test suggests that when complexes interact

with DNA *via* a classical intercalative mode, there is a significant increment in the viscosity of CT-DNA. However, groove or electrostatic binding interactions result in very little perturbation of the DNA viscosity. In order to understand the binding mode, viscosity studies were performed at physiological temperature with varying concentrations of **1** and **2** (from 0 to 140 μM). The relative viscosity (R) of CT-DNA does not show any significant changes on increasing the complex concentration. This result clearly indicates that the complexes do not bind with CT-DNA by an intercalative mode (Fig. 15). Hence the present di and tetranuclear copper complexes bind with CT-DNA *via* electrostatic interactions or a groove binding mode.[46c, d]

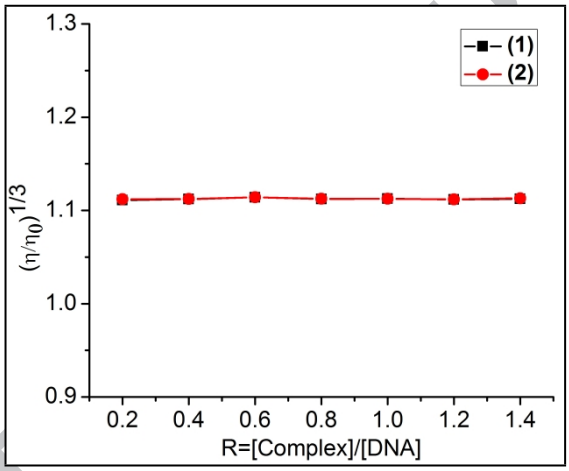

Fig. 15. Effect of increasing amounts of complexes **1** and **2** on the viscosity of CT-DNA. Measurements were performed in 10 mM Tris–HCl buffer, pH 7.4 and at RT with [CT-DNA]= 100 μM; R = [complex]/[CT-DNA]; relative viscosity $(\eta/\eta_0)^{1/3}$ is plotted against R

5.5. Cyclic voltammetric study

Cyclic voltammetric analysis is one of the simple and useful techniques to understand the binding behavior of redox active copper complexes with CT-DNA.[47] The cyclic voltammograms of the copper complexes **1** and **2** in the absence and presence of CT-DNA exhibited considerable shifts in the oxidation and reduction potentials, which indicates that the complexes interact with DNA (Fig. 16, Table 7).

The cyclic voltammetric studies of **1** and **2** were performed with 10 mM Tris-HCl buffer with tetrabutylammonium perchlorate (TBAP) as the supporting electrolyte at pH 7.4 (Fig. 14). Both complexes displayed a quasi-reversible one-electron cathodic peak Epc (reduction potential) at -0.51 and -0.54 V due to the Cu(II)/Cu(I) couple and a one step anodic peak Ea (oxidation potential) at 0.08 and 0.16 V due to the Cu(I)/Cu(II) couple. The obtained potentials matched those of reported copper(II) complexes.[47] M. Jiang *et al*. reported an Epc value of -0.35 V for N,N'-bis(N-hydroxyethylaminoethyl)oxamide bridged binuclear copper(II) complexes[44e] and K. Zheng *et al*. reported a reduction potential Epc at -0.49 V for dinuclear copper(II) complexes with *N*-phenolato-*N*′-[2-(dimethylamino)ethyl]- oxamide ligands.[44f]

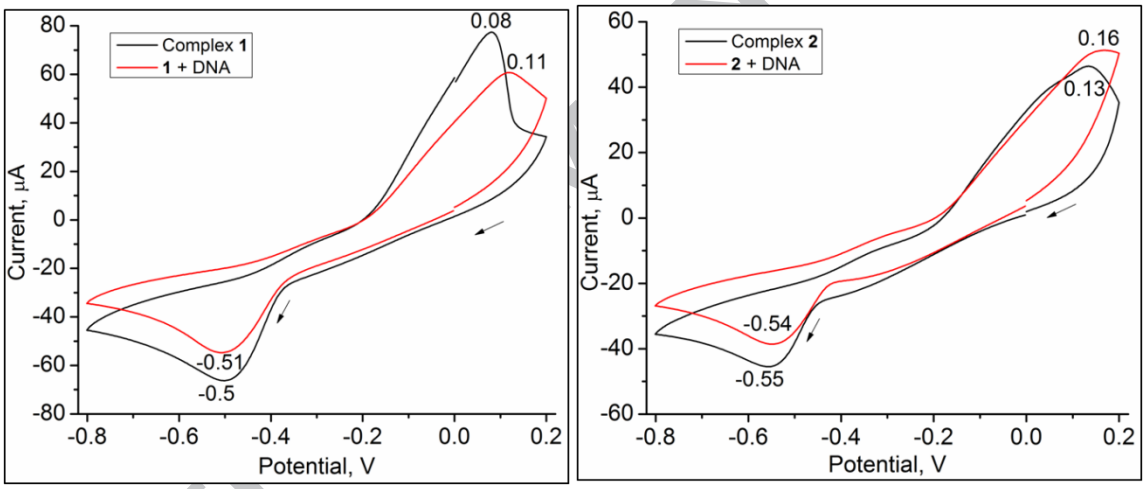

Fig. 16. Cyclic voltammograms of **1** (1 mM) and **2** (0.5 mM) in 10 mM Tris-HCl buffer (pH = 7.4); potentials are referenced *vs* Ag/AgCl; $[Bu_4NClO_4]$ =10 mM; scan rate: 0.05 V s^{-1}.

The ratio of the equilibrium binding constants K_R/K_O was calculated by using the peak change of the initial potential (ΔE^o). Bard and Carter expressed the interaction with small molecules/metal complexes using the simple equation as given below.[49]

$$\Delta E° = E_b° - E_f° - 0.059 \log(K_R/K_O)$$

where $E_f°$ and $E_b°$ are the potentials of the free complex and complex bound with DNA, respectively, and K_{ox} and K_{red} are binding constants for the oxidised and reduced forms with CT-

DNA. The K_{red}/K_{ox} values were 0.98 (**1**) and 1.02 (**2**). The obtained results recommend that both complexes have comparable binding strengths with DNA through groove/electrostatic binding.[25]

Table 7. CV data for complexes **1** and **2**.

	Redox couple	Ipc (A) × 10^{-5}		Epc (V)		$E_{1/2}$ (V)		ΔEp (V)		K_{red}/K_{ox}
		Free	Bound	Free	Bound	Free	Bound	Free	Bound	
1	Cu(II)/Cu(I)	3.65	2.51	-0.50	-0.51	-0.21	-0.20	0.58	0.62	0.98
2	Cu(II)/Cu(I)	1.78	1.73	-0.55	-0.54	-0.21	-0.19	0.68	0.70	1.02

6.1. DNA cleavage studies

The interaction studies of **1** and **2** with supercoiled plasmid DNA (pBR322 DNA) were performed in the absence and presence of reducing agent (ascorbate) by agarose gel electrophoresis. To study the capability of these complexes as DNA cleavage agents, DNA was incubated with different concentrations of **1** and **2** in 50 mM Tris-HCl buffer at pH 7.4 for 2 h and then subjected to gel electrophoresis. The concentration of complex **1** was varied from 0-50 μM, keeping the DNA concentration (0.4 μg) constant. Interestingly, the electrophorogram showed (Fig. 17, lanes 4 and 5) that complex **1** oxidatively cleaves SC (supercoiled circular) DNA to 42% linear DNA (Form III) at 25 μM and 48 % at 50 μM concentration with the reducing agent (Fig. 17, lanes 4 and 5). Complex **1** does not show any significant DNA cleavage in the absence of a reducing agent (lanes 6-8).

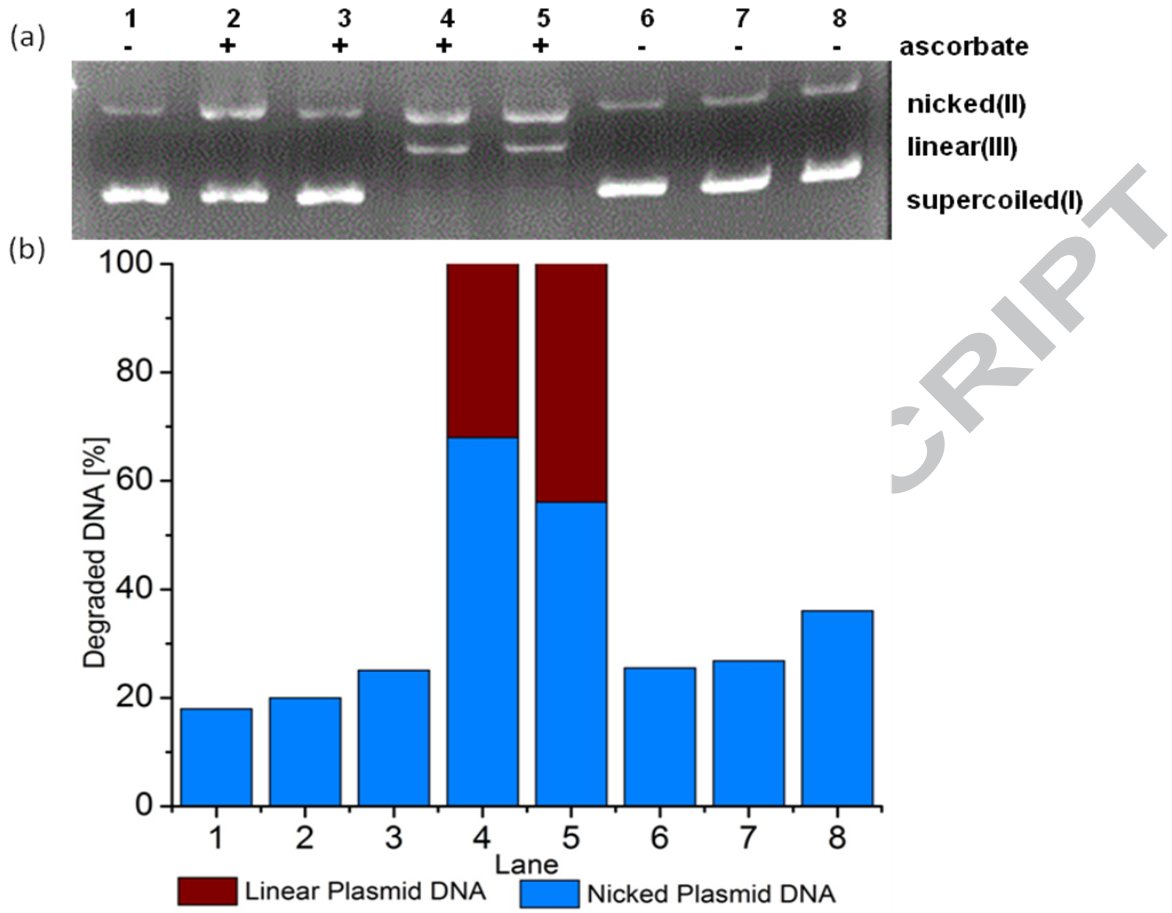

Fig.. 17. (a) Cleavage activity of pBR322 DNA with **1** as determined by gel electrophoresis analysis. Each lane contained 0.4 µg DNA in buffer (pH=7.4). Lane 1: reference DNA; Lane 2: DNA + 1 mM ascorbate; lane 3-5: 1 mM ascorbate + **1** (12.5, 25 and 50 µM, respectively); lane 6-8: **1** (12.5, 25 and 50 µM, respectively). (b) Bar chart representing the percentage of degraded DNA.

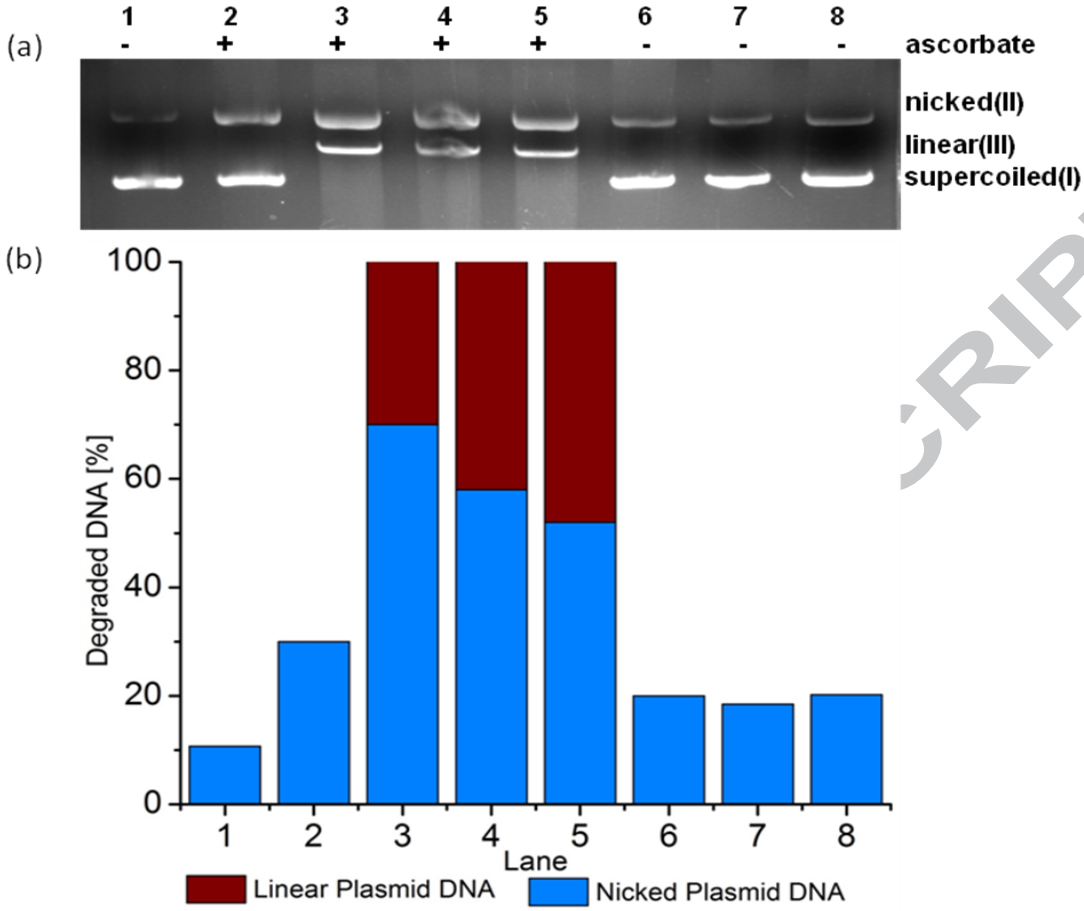

Fig. 18. (a) Cleavage activity of pBR322 DNA with **2** as determined by gel electrophoresis analysis. Each lane contained 0.4 µg DNA in buffer (pH=7.4). Lane 1: reference DNA; Lane 2: DNA + 1 mM ascorbate; lane 3-5: 1 mM ascorbate + **2** (6.25, 12.5 and 25 µM respectively); lane 6-8: **2** (6.25, 12.5 and 25 µM respectively). (b) Bar chart representing the percentage of DNA forms.

Similarly, we performed DNA cleavage studies for complex **2**, the electrophorogram showed (Fig. 18, lanes 3-5) that complex **2** oxidatively cleaves SC (supercoiled circular) DNA to 30% linear plasmid DNA (Form III) at 6.25 µM, 42 % at 12.5 µM and 49 % at 25 µM concentration with a reducing agent (Fig. 18, lanes 3-5). In the absence of a reducing agent, **2** did not cause any significant DNA cleavage (lanes 6-8).

The achieved results were comparable with copper complexes reported by various groups.[50,51] The heteroleptic dinuclear copper(II) complexes of a benzamide based ligand

reported by S. Ramakrishnan *et al*. were able to cleave plasmid DNA to the nicked form at very high concentrations (100 μM).[44d] Dinuclear copper(II) complexes with a bis(benzoyl hydrazone) ligand, demonstrated by R. H. Sabina and his coworkers, were able to cleave plasmid DNA to Form II (nicked) at 10 μM.[50a] Dinuclear copper(II) complexes with a biimidazole ligand, synthesized by Y. Li's research group, showed cleavage activity at 50 μM concentration, whereas the dinuclear copper(II) complexes with a naphthalene-sulfonyl-triazole ligand reported by J. Hernández-Gil *et al*. exhibited cleavage at 30 μM concentration.[51a,b] S. Gama and his coworkers described tridentate pyrazole based dinuclear copper(II) complexes that could cleave plasmid DNA at 50 μM concentration.[51c] The synthesis of dinuclear copper(II) complexes with amidino-O-methylurea ligands was explored by A. Meenongwa *et al*. and these complexes showed cleavage to Form II at 50 μM concentration.[51d] When we compare complexes **1** and **2** with the above examples, both complexes showed good results at very low concentrations (25 μM).

6.2. DNA quenching studies

In order to understand the reactive oxygen species (ROS) responsible for DNA cleavage, quenching studies were done for complexes **1** and **2** with different scavengers, as shown in Fig. 19. These scavengers were tertiary butanol (*tert*-BuOH) and dimethylsulfoxide (DMSO) for hydroxyl radicals, sodium azide (NaN_3) for singlet oxygen, catalase for hydrogen peroxide and superoxide dismutase (SOD) for superoxides. For both compounds **1** and **2**, DNA adduct formation was observed in the presence of catalase, therefore DNA migration was prevented (Fig. 19). The obtained results showed a strong quenching effect by sodium azide for complex **1** (Fig. 19, Lane 6), whereas SOD showed a weak quenching effect and there was no significant change with the other scavengers (Fig. 19, Lane 8). In presence of *tert*-butanol and DMSO,

shearing of DNA was observed (Fig. 19, Lane 4 and 5). Hence singlet oxygen could be the reactive oxygen species responsible for the DNA cleavage by complex **1**. The percentage of each form of DNA in the presence of the scavengers is shown in Fig. 20 for complex **1**. In the case of complex **2**, a weak quenching effect was observed by sodium azide and *tert*-butanol (Fig 21). Hence singlet oxygen and hydroxyl radicals might be the reactive species responsible for DNA cleavage by complex **2**. In the present study, Cu(I) species would be generated by the reaction of the Cu(II) complex with ascorbate (reducing agent), which on reaction with oxygen produces Cu(I)-superoxide, similar to literature reports.[50c,d]

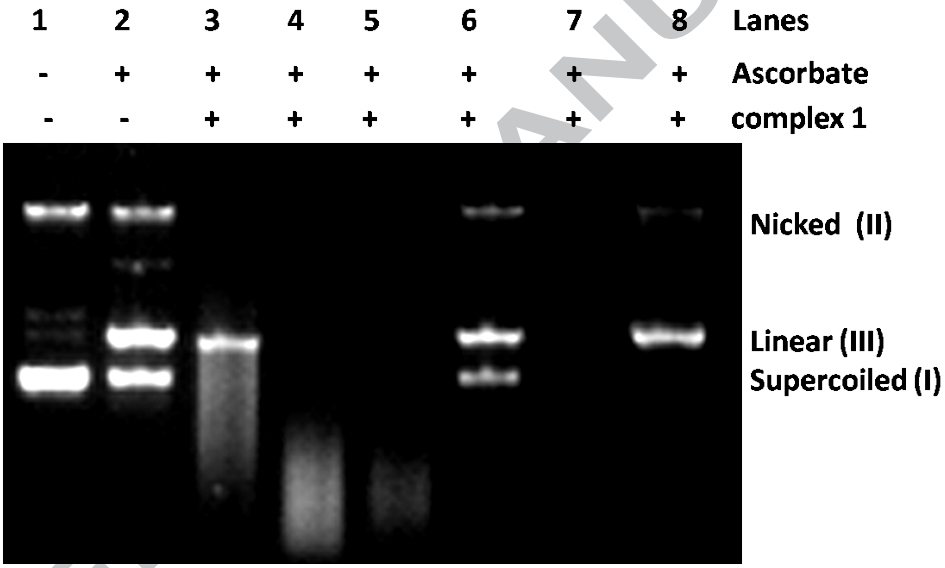

Fig. 19. Quenching effects of DNA cleavage by **1** monitored by 1% agarose gel electrophoresis. Every lane contained 0.4 μg of DNA. Lane 1: reference DNA; Lane 2-8 contained 1 mM ascorbate; Lane 3-8 contained 25 μM of complex **1**; Lane 4: 200 mM *tert*-butanol; Lane 5: 200 mM DMSO; Lane 6: 10 mM sodium azide; Lane 7: 2.5 mg/mL catalase; Lane 8: 5 units of SOD.

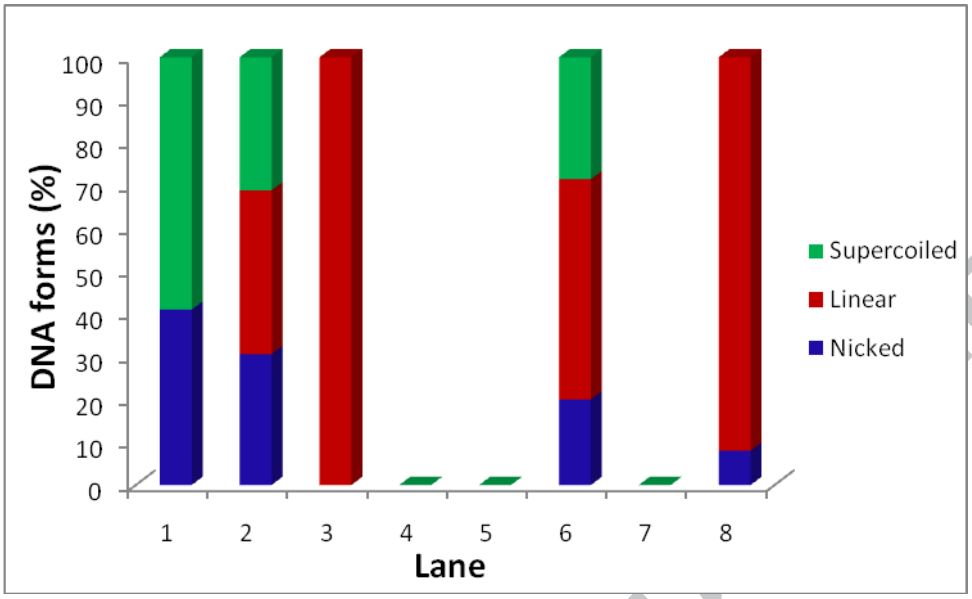

Fig. 20. The % of the degraded form of DNA by complex **1** in the presence of scavengers.

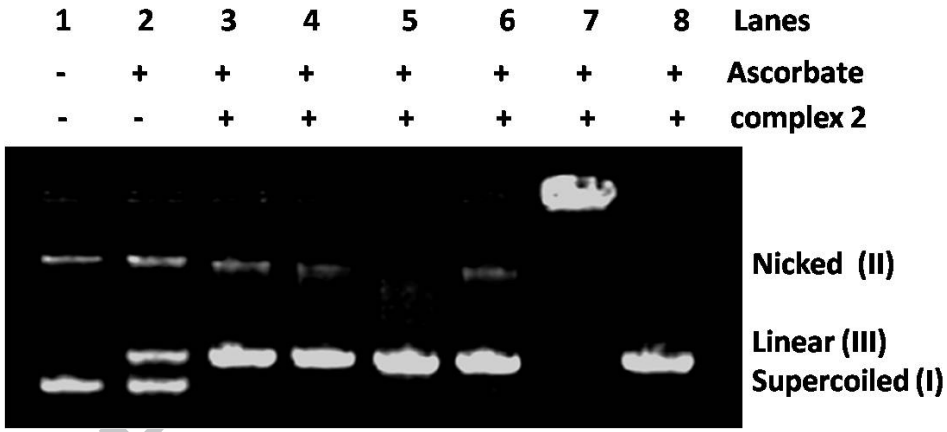

Fig. 21. Quenching effects of DNA cleavage by complex **2** monitored by 1% agarose gel electrophoresis. Every lane contained 0.4 µg of DNA. Lane 1- reference DNA; Lane 2-8 contained 1 mM ascorbate; Lane 3-8 contained 25 µM of complex **2**; Lane 4: 200 mM tertiary butanol; Lane 5: 200 mM DMSO; Lane 6: 10 mM sodium azide; Lane 7: 2.5 mg/mL catalase; Lane 8: 5 units of SOD.

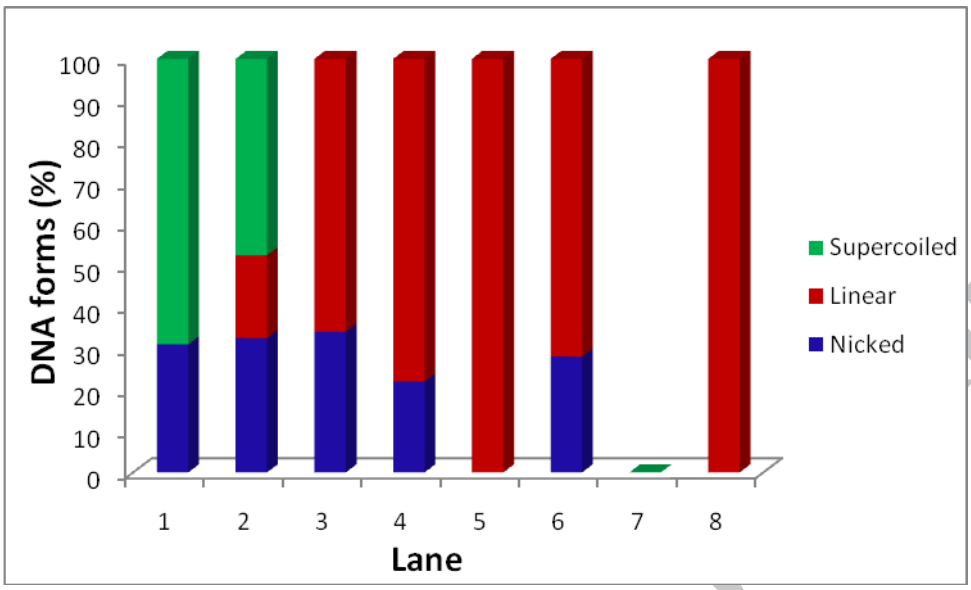

Fig. 22. The % of the degraded form of DNA by complex **2** in the presence of scavengers.

7. Molecular docking with DNA

In silico DNA studies were carried out for complexes **1** and **2** using duplex DNA with the sequence d $(CGCGAATTCGCG)_2$ dodecamer (PDBID:1BNA) in order to understand and interpret the molecular mechanism of the binding interaction with DNA.[52] The minimum energy docked pose of complexes **1** and **2** are depicted in Fig. 23, which revealed that the complexes nicely fit into a major groove binding site.[53] Complex **2** formed a few intermolecular hydrogen bonding interactions with DNA, which provides additional stabilization, whereas complex **1** did not show any additional interactions with DNA. The comparative binding energies of the resulting docked structures of complexes **1** and **2** with DNA were found to be -7.5 and -6.1 KJ mol^{-1}, respectively.

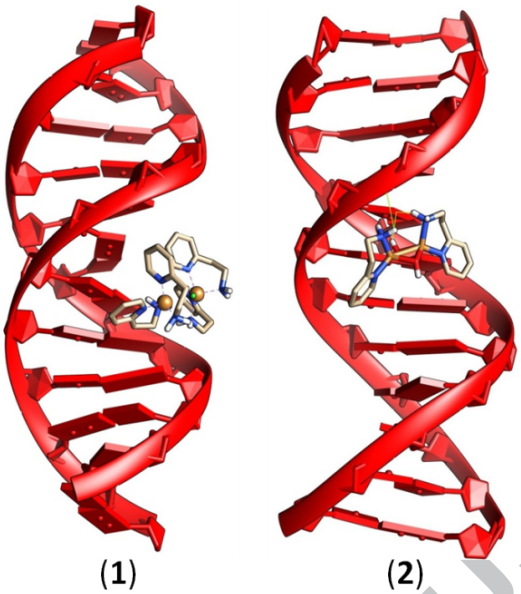

Fig. 23. Best molecular docked pose of complexes (a) **1** and (b) **2** with DNA dodecamer. The duplex sequence is d(CGCGAATTCGCG)$_2$ (PDB ID: 1BNA).

8. Catecholase-like activity

Catechol oxidase (CO) is a type III protein, which catalyzes o-phenols (catechols) to their corresponding o-quinones *via* a two electron oxidation. The active site of these proteins contain two copper centers (Cu-Cu ~ 3.3 Å) in which every copper ion is coordinated by three nitrogen atoms from three histidine moieties.[17-19] Generally, dinuclear copper(II) complexes with Cu···Cu distance of 3-4 Å are used for catalytic studies.[21, 22] 3,5-Ditertiary butyl catechol (3,5-DTBC) has been extensively used as a catalytic model substrate for catecholase-like activity, as it can be easily converted into the corresponding quinone (3,5-DTBQ) in the presence of O_2. The oxidation of 3,5-DTBC can be monitored by UV-Vis spectroscopy, by observing a characteristic DTBQ band at around 400 nm (ε = 1900 M^{-1} cm^{-1}).[19-21]

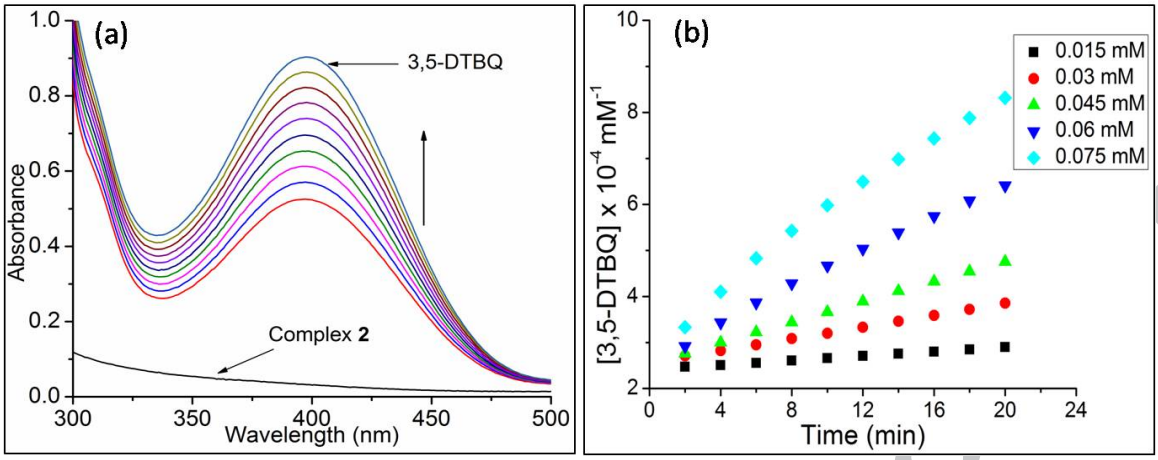

Fig. 24.(a) Absorption spectra showing the increase of the o-quinone band at 398 nm with complex **2** (0.045 mM) in DMF. (b) Plot of [DTBQ] *vs* time for varying concentrations of **2** (0.015-0.075 mM).

In the present work, the kinetic study (Fig. 24) of complexes **1** and **2** was performed by the initial rate method, increasing the absorption of 3,5-DTBQ at around 400 nm every 2 min. A linear relationship between the copper(II) complex concentration and the initial rate was observed, which means a first order dependence on the catalyst concentration with k = 1.47 × 10^{-3} mM s^{-1} (**1**) and 3.45 × 10^{-3} mM s^{-1} (**2**). At high substrate concentrations, saturation kinetics were observed.[19-22] The kinetic parameters V_{max}, k_M and k_{cat} for **1** and **2** were calculated by using both the Michaelis–Menten equation (Fig. 25) and the Lineweaver–Burk method, the results of which are listed in Table 8. The present complexes showed activity comparable with other Cu(II) complexes.[42]

Table 8. K_M, V_{max} and k_{cat} values for complexes **1** and **2**.

Complex	**V_{max} (M s^{-1})**	**K_M (M)**	**k_{cat} (s^{-1})**
$[Cu_2(2\text{-AEP})_4(\mu\text{-Cl})](ClO_4)_2$ (**1**)	5.1× 10^{-3}	0.78× 10^{-3}	5.1 × 10^{-2}
$[Cu_4(\mu_3\text{-OH})_2(\mu_2\text{-OH})_2(2\text{-AEP})_4(\mu_2\text{-}ClO_4)_2](ClO_4)_2$ (**2**)	2.4× 10^{-3}	0.53× 10^{-3}	4.88 × 10^{-2}

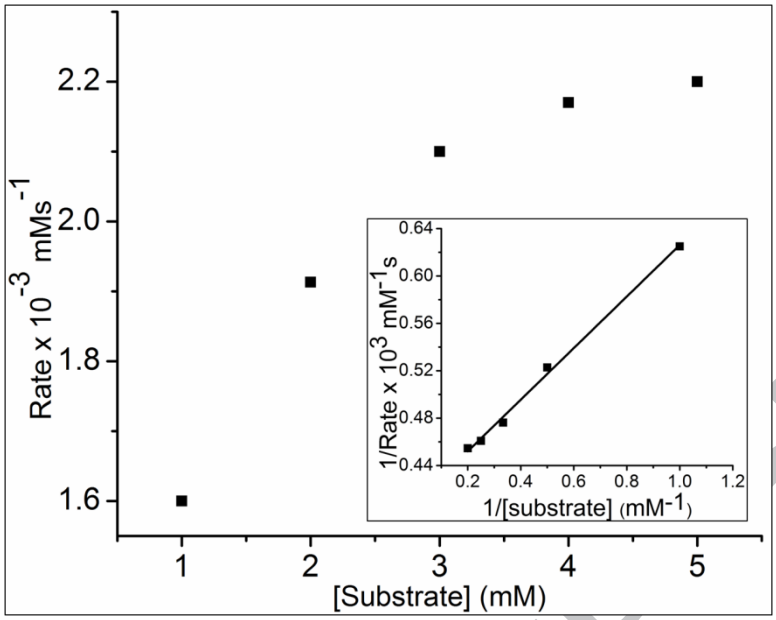

Fig. 25. Saturation kinetics for the oxidation of 3,5-DTBC by complex **2**. Inset illustrates the reciprocal Lineweaver–Burk plot.

9. Cytotoxicity studies

In order to understand the *in vitro* anti cancer activity of the copper complexes **1** and **2**, tests were screened against Human Cervical ME-180 and Cervical SiHa cancer cell lines in comparison to adriamycin (ADR) at the Pharmacology Unit of Advanced Centre for Treatment, Research and Education in Cancer (ACTREC) according to the method by Skehan *et al*.[55] The GI_{50} value was defined as the concentration of drug causing 50% inhibition of cell growth, and these values are presented in Table 9. Complex **1** displayed a better anticancer activity against both cell lines (ME-180 and SiHa) compared to complex **2**. These results showed moderate activities which were comparable with reported copper(II) complexes.[56]

Table 9. *In vitro* GI_{50} of complexes **1** and **2**

Complex	**GI_{50} (μM) (μg/mL)**	
	ME-180	**SiHa**
$[Cu_2(2\text{-}AEP)_4(\mu\text{-}Cl)](ClO_4)_2$ (**1**)	31.30	44.45
$[Cu_4(\mu_3\text{-}OH)_2(\mu_2\text{-}OH)_2(2\text{-}AEP)_4(\mu_2\text{-}ClO_4)_2](ClO_4)_2$ (**2**)	75.30	49.33

ADR	<0.10	<0.10

10. Conclusions

Di and tetranuclear copper(II) complexes with a simple 2-aminoethyl pyridine ligand were successfully synthesized and completely characterized by elemental analysis, electrochemical, spectroscopic and single crystal XRD techniques. The dinuclear complex **1** showed a distorted square pyramidal geometry around both copper centers. The tetranuclear complex **2** displayed a distorted square pyramidal geometry around two coppers centres and an octahedral geometry at the other two copper centers. Complex **1** has a rarely observed single chloro bridge between the dicopper centers. Both complexes showed the possibility of ferromagnetic and antiferromagnetic interactions with +J and –J values. The complexes efficiently hydrolysed the phosphodiester BNPP. A DNA *in silico* study suggested that both copper(II) complexes could bind with CT-DNA *via* a major groove mode, which was further confirmed by UV-Vis spectral titration, electrochemical analysis, circular dichroism measurements and viscosity studies. The binding strength of complex **1** showed a higher propensity than **2** with CT-DNA by docking studies. Both complexes showed efficient DNA cleavage activities at very low concentrations (25 μM) to form III. The catecholase activity of these complexes were investigated and complex **2** showed better activity than **1**. The complexes showed moderate anticancer activity against ME-180 and SiHa cervical cancer cell lines.

11. Experimental section

11.1. Materials

The Cu(II) salts (copper(II) perchlorate hexahydrate and copper(II) chloride dihydrate) and other the chemicals, 2-animoethylpyridine, triethylamine, sodium perchlorate, bis(4-nitrophenyl) phosphate, 3,5-ditertiarybutyl catechol, calf-thymus DNA and supercoiled plasmid

DNA, were commercially available and used as received. Solvents were dried and distilled by standard procedures.[57] All reagent grade compounds were used without further purification.

11.2. Physical measurements

UV-Vis spectra were recorded on a UV-2450 spectrophotometer and FT-IR spectra were obtained on a Shimadzu IR-470 spectrophotometer. C, H and N elemental analysis data was carried out on a Thermo Scientific FLASH 2000 Organic Elemental Analyzer and EPR spectra were obtained on a Varian E-112 model X-band instrument. CD spectral data were performed on a JASCO J-815 CD spectrometer. Viscosity studies were performed on an Ostwald Viscometer.

11.3. Magnetic measurements

Powdered crystalline samples of complexes **1** and **2** were used with a Quantum Design® SQUID magnetometer to get the magnetic susceptibility data. The molar magnetic susceptibility χ_M was analyzed in the temperature range 2-300 K. Pascal's constants were used to calculate the corrections for the diamagnetic response of the samples.[58]

11.4. BNPP hydrolysis study

The hydrolysis of BNPP was performed by using UV-vis spectroscopy at pH 8.4 and under physiological conditions. The formation of para nitrophenol was measured by the initial slope method. The complex and BNPP concentrations used for this study were as follows: 0.0088 mM (**1**), 0.0176 mM (BNPP); 0.0069 mM (**2**), 0.0276 mM (BNPP).

11.5. DNA interaction studies

11.5.1. UV-Vis spectrophotometric study

Binding interaction studies were performed at ambient temperature using a Shimadzu spectrophotometer (UV-2450 model) with a 1 cm pathlength rectangular quartz cuvette. A CT-DNA stock solution was prepared from 10 mM Tris–HCl buffer (pH = 7.4) and the concentration of CT-DNA was calculated at 260 nm with $\varepsilon = 6600\ M^{-1}\ cm^{-1}$.[59] The buffer solution of CT-DNA

showed a band ratio at 260 and 280 nm of around 1.8–1.9, which clearly demonstrates that the CT-DNA was adequately free from protein. The concentration of the complexes was kept constant and the CT-DNA concentration was augmented from 0–20 mM.

11.5.2. FT-IR spectrometric study

In order to identify which nucleotides of CT-DNA were interacting with the copper complexes, IR spectra were performed on a SHIMADZU IR spectrophotometer. The CT-DNA (0.2 mM) and copper complexes (1 mM) were dissolved in 10 mM Tris-HCl buffer solution. The spectra were recorded after 1 h incubation at 25 °C, using KBr pellets.

11.5.3. CD spectroscopic study

CD spectroscopy is one of the useful techniques to gain understanding of whether any conformation change in CT-DNA occurs after binding with metal complexes. This study was carried out at ambient temperature on a Jasco model (J-720) spectropolarimeter with a 10 mm pathlength cylindrical quartz cuvette. Initially a CD spectrum was recorded for free CT-DNA (100 μM concentration) in the wavelength range 220–320 nm. Next, CD spectra for the complexes and DNA at 50 μM were recorded, which are illustrated in Fig. 14.

11.5.4. Viscosity measurements

The viscosity studies were carried out using an Ostwald Viscometer at room temperature. In order to find the viscosity of the solution, 15 mL of a 10 mM Tris–HCl buffered solution and 100 μM of CT-DNA were taken in the viscometer and a flow time reading was measured. Further, the CT-DNA concentration was kept constant and an appropriate amount of the complexes (0-140 μM**)** was added to the viscometer to give a certain ratio value and the flow time was recorded. The obtained data were plotted as the relative viscosity $(\eta/\eta_o)^{1/3}$ *vs* R, where η and η_o are the specific viscosity of DNA in the presence and absence of the complexes. The measurements were done three times and the average value was used for the calculations.

11.6. DNA cleavage studies

Plasmid DNA cleavage studies of the copper(II) complexes **1** and **2** were carried out with 0.4 μg supercoiled pBR322 DNA by agarose gel electrophorosis. The complex solutions were prepared in 10 mM Tris-HCl buffer solution (pH = 7.4) at RT, incubated for 2 hours. After incubation, the pBR322 DNA and complex samples were placed on horizontal agarose gels (1%) containing ethidium bromide (2 μg/mL) in 0.5 × Tris base-boric acid-EDTA (TBE) buffer for 2 h at 40 V. Quantification of the closed Form-I (circular-DNA), Form II (nicked-DNA) and Form III (linear-DNA) was made *via* analysis of EB and the samples containing agarose gels by a fluorescence instrument (*Bio-Rad* Gel Doc EZ Imager). The obtained results were analyzed with Image Lab 3.0 software. DNA cleavage analyses were performed three times and the standard is shown in the bar diagrams.

DNA cleavage inhibition studies

DNA samples (0.4 μg) were prepared in 50 mM Tris-HCl buffer (pH 7.4) and incubated at RT for 2 h. DNA samples were run by horizontal agarose gel electrophoresis using 1% gel containing 2 μg/mL of ethidium bromide in 1X TAE buffer for 1 h at 50 V. DNA was incubated under the same conditions as described above in the presence of 200 mM tertiary butanol, 200 mM dimethyl sulfoxide (DMSO), 10 mM sodium azide, 2.5 mg/mL catalase and 5 units of superoxide dismutase (SOD). Catalase was prepared in PBS and pre-incubated at 37 °C for 30 min. The same PBS concentration was maintained in every incubation mixture. DNA was visualized using the gel documentation system (Bio-Rad Universal Hood II) and the percentage of the closed circular, nicked/relaxed and linear DNA forms was determined.

11.7. Molecular docking

The binding interactions of complexes **1** and **2** with duplex DNA were measured by rigid molecular *in silico* studies using Auto dock 4.2 software. This software is convenient and an

interactive computer based program to understand drug-DNA binding interactions. The structures of the copper(II) complexes were sketched by Chem Bio Draw Ultra 13, saved as mol format and OPEN BABEL (http://www.vcclab.org/lab/babel/) software was used to convert from mol formate to pdb format. The dodecamer B-DNA was used for the docking studies, which has the sequence $(CGCGAATTCGCG)_2$ (PDB ID:1BNA), and was downloaded from the Protein Data Bank (PDB) (http://www.rcsb.org./pdb).[60]

11.8. Single crystal XRD analysis

Single crystal X-ray studies were carried out on an X calibur Oxford Diffraction Ltd. instrument with Mo-Kα radiation (λ = 0.71073 Å). Structure refinement and analysis were carried out with SHELX-97.[61] All non-H atoms were refined anisotropically and were generated according to the stereochemistry and refined using same model software. X-ray crystal data and structure refinement parameters are shown in Table 1. Both complexes showed disorders in the crystal structures, especially with perchlorate ions and methylene groups of the 2-AEP ligands.

11.9. Synthesis of the metal complexes

11.9.1. Synthesis of $[Cu(2\text{-}AEP)_4(\mu\text{-}Cl)](ClO_4)_3$ (1)

An ethanolic solution (1 mL) of the ligand 2-AEP (0.122 g, 1 mmol) was added to an ethanolic (3 mL) solution of copper(II) chloride dihydrate (0.17 g, 1 mmol). To this blue colored solution, triethylamine (NEt_3) (0.303 g, 3 mmol) was added and the resultant solution was stirred for 2 h at room temperature. Finally sodium perchlorate monohydrate (0.14 g, 1 mmol) ($NaClO_4.H_2O$) was added and no color change was observed. This suspension was stirred for one hour at room temperature. A blue colored precipitate was filtered off and dried under reduced pressure to yield **1** (0.427 g, 45%). X-ray quality crystals were obtained by slow evaporation of a solution of complex **1** in a mixture of acetonitrile/methanol. Anal. Calcd. for $C_{28}H_{40}Cl_4Cu_2N_8O_{12}$ (M.wt = 949.56 g mol^{-1}) calcd: C 35.42; H 4.25; N 11.80; Found: C 35.59; H 4.27; N 11.94%.

UV-Vis (DMF, nm) λ_{max}: 735 (ε = 206 M^{-1} cm^{-1}). FT-IR (KBr, cm^{-1}): 3314-3447 (ν_{N-H} stretching); 3140-3214 ($\nu_{C=C-H}$ stretching); 2917 (ν_{C-H} stretching); 1088 (bs), 623 (s) $\nu(ClO_4)$.

11.9.2. Synthesis of $[Cu_4(2\text{-AEP})_4(\mu_2\text{-}OH)_4(\mu_2\text{-}ClO_4)_2]ClO_4)_2$ (2)

A solution of the ligand 2-AEP (0.122 g, 1 mmol) in ethanol (1 mL) was added to a solution of copper perchlorate hexahydrate (0.37 g, 1 mmol) in the same solvent (3 mL). To the obtained light blue colored solution was added triethylamine (NEt_3) (0.303 g 3 mmol), resulting in a blue colored precipitate, which was stirred for 2 h, filtered and dried under reduced pressure to yield **2** (0.421 g, 70%). X-ray quality crystals were obtained by slow evaporation of a solution of complex **2** in acetonitrile. Anal. Calcd. for $C_{28}H_{44}Cl_4Cu_4N_8O_{20}$ (M.wt = 1208.68 g mol^{-1}) calcd: C 27.82; H 3.67; N 9.27; Found: C 28.04; H 3.81; N 9.35%. UV-Vis (DMF, nm) λ_{max}: 608 (ε = 147 M^{-1} cm^{-1}). FT-IR (KBr, cm^{-1}): 3482 (ν_{O-H} stretching); 3405 (ν_{N-H} stretching); 3107-3190 ($\nu_{C=C-H}$ stretching); 2924 (ν_{C-H} stretching); 1080 (bs), 630 (s) $\nu_{(ClO4)}$.

Acknowledgments

We are thankful to Pondicherry University for the start-up grant project. P. S thanks the CSIR, New Delhi for SRF. S. S and P. S thank DST-FIST for the S-XRD facility.

References

1. S. Youngme, G.A.V. Albada, H. Kooijman, O. Roubeau, W. Somjitsripunya, A.L. Spek, C. Pakawatchai, J. Reedijk, Eur. J. Inorg. Chem. (2002) 2367.
2. S.S. Massoud, M. Spell, C.C. Ledet, T. Junk, R. Herchel, R.C. Fischer, Z. Trávníček, F. A. Mautne, Dalton Trans. 44 (2015) 2110.
3. S. Balboa, R. Carballo, A. Castiñeiras, J. M. González-Pérez, J. Niclós-Gutiérrez, Polyhedron 27 (2008) 2921.
4. (a) J.A. Cowan, Curr. Opin. Chem. Biol. 5 (2001) 634; (b) P.B. Dervan, Science 232 (1986) 464.
5. C. Hemmert, M.P.M. Renz, H. Gornitzka, S.S.B. Meunier, J. Biol. Inorg. Chem. 6 (2001) 14.
6. D.M. Perreault, E.V. Anslyn, Angew. Chem. Int. Ed. 36 (1997) 432.

7. (a) K.A. Deal, G. Park, J. Shao, N.D. Chasteen, M.W. Brechbiel, R.P. Planalp, Inorg. Chem. 40 (2001) 4176; (b) (c) K.M. Deck, T.A. Tseng, J.N. Burstyn, Inorg. Chem. 41 (2002) 669.
8. (a) S. Sabiah, B. Varghese, N.N. Murthy, Chem. Commun. (2009) 5636; (b) L. Tjioe, T. Joshi, C.M. Forsyth, B. Moubaraki, K.S. Murray, J. Brugger, B. Graham, L. Spiccia, Inorg. Chem. 51 (2012) 939.
9. F.H. Fry, A.J. Fischmann, M.J. Belousoff, L. Spiccia, J. Brugger, Inorg. Chem. 44 (2005) 941.
10. G. Evano, N. Blanchard, M. Toumi, Chem. Rev. 108 (2008) 3054.
11. C. Santini, M. Pellei, V. Gandin, M. Porchia, F. Tisato, C. Marzano, Chem. Rev. 114 (2014) 815.
12. J.D. Ranford, P.J. Sadler, D.A. Tocherb, J. Chem. Soc. ,Dalton Trans. (1993) 3393.
13. G.D. Munno, M. Julve, F. Lloret, J. Faus, M. Verdaguer, A. Caneschi, Angew. Chem. Int. Ed. 32 (1993) 1046.
14. R. Singh, F. Lloret, R. Mukherjee, Z. Anorg. Allg. Chem. 640 (2014) 1086.
15. I. Nazarenko, F. Pop, Q. Sun, A. Hauser, F. Lloret, M. Julve, A. El-Ghayoury, N. Avarvari, Dalton Trans. 44 (2015) 8855.
16. S.J. Smith, C.J. Noble, R.C. Palmer, G.R. Hanson, G. Schenk, L.R. Gahan, M.J. Riley, J. Biol. Inorg. Chem. 13 (2008) 499.
17. A. Banerjee, S. Sarkar, D. Chopra, E. Colacio, K.K. Rajak, Inorg. Chem. 47 (2008) 4023.
18. E.I. Solomon, U.M. Sundaram, T.E. Machonkin, Chem. Rev. 96 (1996) 2563.
19. P.K. Nanda, V. Bertolasi, G. Aromí, D. Ray, Polyhedron 28 (2009) 987.
20. A. Majumder, S. Goswami, S.R. Batten, M.S. Fallah, J. Ribas, S. Mitra, Inorg. Chim. Acta 359 (2006) 2375.
21. M. Thirumavalavan, P. Akilan, M. Kandaswamy, G. Chinnakali, G. Senthil Kumar, H.K. Fun, Inorg. Chem. 42 (2003) 3308.
22. S. Majumder, S. Sarkar, S. Sujit, S.E. Carolina, M. Sasankasekhar, Inorg. Chem. 50 (2011) 7540.
23. (a) K. Jitsukawa, M. Mizutani, H. Arii, I. Kubo, Y. Izu, T. Ozawa, H. Masuda, Chem. Lett. 33 (2004) 1302; (b) B.A. Gandhi, O. Green, J.N. Burstyn, Inorg.Chem. 46 (2007) 3816; (c) Z Yuan, G.-C. Kuang, R.J. Clark, L. Zhu, Org. Lett. 14 (2012) 2590; (d) M. Pasquali, C. Floriani, A. Gaetani-Manfredotti, Inorg. Chem. 20 (1981) 3382; (e) E.H. Alilou, M. Giorgi,

M. Pierrot, M. Reglier Acta Crystallogr. C. C48 (1992) 1612; (f) R.A. Bream, E.D. Estes, D.J. Hodgsos, Inorg. Chem. 14 (1975) 1672; (g) K.-B. Huang, Z.-F. Chen, Y.-C. Liu, M. Wang, J.-H. Wei,X.-L. Xie, J.-L. Zhang, K. Hu, H. Liang, Eur. J. Med. Chem. 70 (2013) 640; (h) A. Wojtczak, M. Jaskolski, Z. Kosturkiewicz, Acta Crystallogr. C. C43 (1987) 645.

24. A.W. Addison, T.N. Rao, J. Reedijk, J. van Rijn, G.C. Verschoor, Dalton Trans. (1984) 1349.
25. E.P. McMoran, D.R. Powell, F. Perez, G.T. Rowe, L. Yang, Inorg. Chem. 55 (2016) 11462.
26. R. D. Köhn, Z. Pan, M. F. Mahon, G. Kociok-Köhn, Dalton Trans. (2003) 2269.
27. S. Putzien, S. Wirth, J. N. Roedel, I.-P. Lorenz, Polyhedron 30 (2011) 1747.
28. M. Jagadeesh, K.K. Suresh, L. Sivarama Krishna, A.V. Reddy, Spectrochim. Acta Part A. 118 (2014) 552.
29. T.M. Dunn, 1960 *The visible and ultraviolet spectra of complex compounds in modern coordination chemistry* (New York: Interscience).
30. A.Yan, T. Ming-Liang, J. Liang-Nian, M. Zong-Wan, Dalton Trans. (2006) 2066.
31. L.P. Battaglia, A.B. Corradi, L. Menabue, G.C. Pellacani, J. Chem. Soc., Dalton Trans. (1981) 8.
32. A.K. Patra, M. Nethaji, A.R. Chakravarty, J. Inorg. Biochem. 101 (2007) 233.
33. (a) X. Li, D. Cheng, J. Lin, Z. Li, Y. Zheng, Cryst. Growth Des. 8 (2008) 2853; (b) Y.–Q. Zheng, D.–Y. Cheng, B.–B. Liu, W.–X. Huang, Dalton Trans. 40 (2011) 277; (c) G. A. V. Albada, I. Mutikainen, O. Roubeau, U. Turpeinen, J. Reedijk, Inorg. Chim. Acta 331 (2002) 208; (d) X.-F. Wang, K.-J. Du, H.-Q. Wang, X.-L. Zhang, C.-M. Nie, J. Mol. Struct. 1138 (2017) 155; (e) J. Sletten, A. Sørensen, M. Julve, Y. Journaux, Inorg. Chem. 29 (1990) 5054.
34. (a) I.A. Koval, D. Pursche, A.F. Stassen, P. Gamez, B. Krebs, J. Reedijk, Eur. J. Inorg. Chem. (2003) 1669; (b) B. Apurba, K.D. Lakshmi, G.B.D. Michael, D. Carmen, G. Ashutosh, Inorg. Chem. 51 (2012) 10111; (c) R. Papadakis, E. Riviere, M.Giorgi, H. Jamet, P. Rousselot-Pailley, M. Reglier, A. J. Simaan, T. Tron, Inorg. Chem. 52 (2013) 5824.
35. R. Singh, F. Lloret, R. Mukherjee, Z. Anorg. Allg. Chem. 640 (2014) 1086.
36. D.L. Reger, A.E. Pascui, E.A. Foley, M.D. Smith, Inorg. Chem. 56 (2017) 2884.
37. I. Castro, M. JuIve, G.D. Munno, G. Bruno, J.A. Real, F. Lloret, J. Faus, J. Chem. Soc., Dalton Trans. (1992) 1739.
38. J.A. Barnes, D.J. Hodgson, W.E. Hatfield, Inorg. Chem. 11 (1972) 144.

39. V.H. Crawford, H.W. Richardson, J.R.Wasson, D.J. Hodgson, W.E. Hatfield, Inorg. Chem. 15 (1976) 2107.

40. E. Ruiz, P. Alemany, S. Alvarez, J. Cano, Inorg. Chem. 36 (1997) 3683.

41. W. Le, Y. Yong, L. Vasiliki, A. Alexander, M. Li-June, Z. Yufen, Eur. J. Inorg. Chem. (2011) 674.

42. (a) E.L. Hegg, S.H. Mortimore, C.L. Cheung, J.E. Huyett, D.R. Powell, J.N. Burstyn, Inorg. Chem. 38 (1999) 2961; (b) R.E.H.M.B. Osaório, Inorg. Chem. 51 (2012) 1569.

43. M. Roy, S. Dhar, B. Maity, A.R. Chakravarty, Inorg. Chim. Acta 375 (2011) 173.

44. (a) N.M.R. Martins, S. Anbu, K.T. Mahmudov, R. Ravishankaran, M.F.C.G. Silva, L.M.D. R.S. Martins, A.A. Karande, A.J.L. Pombeiro, New J. Chem. 41 (2017) 4076; (b) Q.-Q. Zhang, F. Zhang, W.-G. Wang, X.-L. Wang, J. Inorg. Biochem. 100 (2006) 1344; (c) J. He, J. Sun, Z.W. Mao, L.N. Ji, H. Sun, J. Inorg. Biochem. 103 (2009) 851; (d) S. Ramakrishnan, D. Shakthipriya, E. Suresh, V. Periasamy, M.A. Akbarsha, M. Palaniandavar, Inorg. Chem. 50 (2011) 6458; (e) M. Jiang, Y.-T. Li, Z.-Y. Wu, Z.-Q. Liu, C.-W. Yan, J. Inorg. Biochem. 103 (2009) 833; (f) K. Zheng, F. Liu, X.-M. Xu, Y.-T. Li, Z.-Y. Wu, C.-W. Yan, New J. Chem. 38 (2014) 2964; (g) F.-H. He, L. Tao, X.-W. Li, Y.-T. Li, Z.-Y. Wu, C.-W. Yan, New J. Chem. 36 (2012) 2078.

45. (a). A.A. Ouameur, H-A. Tajmir-Riahi, J. Biol. Chem. 279 (2004) 42041. (b). D.K. Jangir, G. Tyagi, R. Mehrotra, S. Kundu, J. Mol. Struct. 969 (2010) 126; (c). D.M. Loprete, Biochemistry 32 (1993) 4077.

46. (a) D.-D. Li, J.-L. Tian, W. Gu, X. Liu, S.-P. Yan, Eur. J. Inorg. Chem. (2009) 5036; (b) R. Loganathan, S. Ramakrishnan, E. Suresh, A. Riyasdeen, M.A. Akbarsha, M. Palaniandavar, Inorg. Chem. 51 (2012) 5512.(c) P. Sureshbabu, A. A. J. S. Tjakraatmadja, C. Hanmandlu, K. Elavarasan, N. Kulak, S. Sabiah, RSC Adv. 5 (2015) 22405; (d) J.-H. Shi, J. Chen, J. Wang, Y.-Y. Zhu, Spectrochim. Acta Part A 136 (2015) 443.

47. M. Jianga, Y.-T. Li, Z.-Y. Wu, Z.-Q. Liu, C.-W. Yan, J. Inorg. Biochem. 103 (2009) 833.

48. M.T. Carter, M. Rodriguez, A.J. Bard, J. Am. Chem. Soc. 111 (1989) 8901.

49. M.T. Carter, A.J. Bard, J. Am. Chem. Soc. 109 (1987) 7528.

50. (a) R.-H. Sabina, W. Christian, B.L. Ana, C. Rosa, N. Kulak, M.V.-L. Ezequiel, Eur. J. Inorg. Chem. (2013) 5843; (b) W. Christian, L. Carsten, N. Kulak, Eur. J. Inorg. Chem. (2014)

2597. (c) D.S. Sigman, Acc. Chem. Res., 19 (1986) 180; (d) J.E. Baiglow, A.V. Kachur, Radiat. Res., 48 (1997) 181.

51. (a) Y. Li, Y. Wu, J. Zhao, P. Yang, J. Inorg. Biochem. 101 (2007) 283; (b) J. Hernández-Gil, S. Ferrer, N. Cabedo, M.P. López-Gresa, A. Castiñeiras, F. Lloret, J. Inorg. Biochem. 125 (2013) 50; (c) S. Gama, F. Mendes, F. Marques, I.C. Santos, M.F. Carvalho, I. Correia, J.C. Pessoa, I. Santos, A. Paulo, J. Inorg. Biochem. 105 (2011) 637; (d) A. Meenongwa, R.F. Brissos, C. Soikum, P. Chaveerach, P. Gamez, Y. Trongpanich, U. Chaveerach, New J. Chem. 39 (2015) 664.
52. R. Rohs, I. Bloch, H. Sklenar, Z. Shakked, Nucleic Acids Res. 33 (2005) 7048.
53. (a) R. Filosa, A. Peduto, S. Di Micco, P.D. Caprariis, M. Festa, A. Petrella, G. Capranico, G. Bifulco, Bioorg. Med. Chem. 17 (2009) 13.
54. M. Shamsi, S. Yadav, F. Arjmand, J. Photochem. Photobiol. B, Biol. 136 (2014) 1.
55. P. Skehan, R. Storeng, D. Scudiero, A. Monks, J. McMahon, D. Vistica, J.T. Warren, H. Bokesch, S. Kenney, M.R. Boyd, J. Natl. Cancer Inst. 82 (1990) 1107.
56. B.J.M.L. Ferreira, P. Brandão, M. Meireles F. Martel, A. Correia-Branco, D.M. Fernandes, T.M. Santos, V. Félix, J. Inorg. Biochem. 161 (2016) 9.
57. D.D. Perrin, W.L. Armarego, D.R. Perrin, *Purification of Laboratory Chemicals*, Pergamon, New York, 2nd edn, 1980.
58. (a) C.J. O'Connor, Inorg. Chem. 29 (1982) 203; (b) G.A. Bain, J.F. Berry, Diamagnetic Corrections and Pascal's Constants. J. Chem. Educ. 85 (2008) 532.
59. Y. Gultneh, A.R. Khan, D. Blaise, S. Chaudhry, B. Ahvani, B.B. Marvey, R.J. Butcher, J. Inorg. Biochem. 75 (1999) 7.
60. R. Rohs, I. Bloch, H. Sklenar, Z. Shakked, Nucleic Acids Res. 33 (2005) 7048.
61. A. Altomare, G. Cascarano, C. Giacovazzo, A. Guagliardi, J. Appl. Crystallor. 23 (1993) 343.